Role of the Bone Morphogenetic Protein Pathway in Definitive Endoderm Patterning

Carla Gonçalves
Biologia Celular e Molecular
Departamento de Biologia
2015

Orientadores
Professora Anne Grapin-Botton, DanStem, Universidade de Copenhaga
Doutora Laurence Lemaire, DanStem, Universidade de Copenhaga

Coorientador
Professor José Pissarra, Faculdade de Biologia, Universidade do Porto

Todas as correções determinadas pelo júri, e só essas, foram efetuadas.

O Presidente do Júri,

Porto, ____/____/_____

Acknowledgements

As my first year at DanStem comes to an end, it seems awfully hard to address all the people that helped me make this work a reality. First and foremost, I have to thank Anne, because she believed in me from the start and has always been inspiring as a scientist and as a person. I feel so lucky to work with her. Next, I have to thank Laurence for all her invaluable help in and out of the bench. She was always invested in my project, even if her work was already so much to take. I want to thank all the members of the Grapin-Botton group for discussions, advice, for making me grow so much overall as a scientist. And to everyone in DanStem, thank you for making this place so wonderful to work in, thank you for making me feel welcome and thank you for your science!

Agora em português, para os portugueses. Primeiro de tudo, agradeço aos meus pais por me terem ensinado a ser inquisidora e confiante, capacidades tão importantes para um cientista. Os meus pais que tão bem souberam dar-me asas para voar e mostrar-me um mundo a conquistar. Agradeço a todos os meus queridos amigos, quase irmãos, que me acompanharam através de lágrimas, sorrisos e suor. Não há palavras suficientes para explicar a saudade que senti durante este ano. E por último, não porque menos importante, quero agradecer ao Ricardo. Ele que sempre soube fazer-me sorrir quando não parecia possível, mesmo a milhares de quilómetros de distância.

Table of Contents

Resumo

A Endoderme Definitiva (DE) é uma das três camadas germinativas formadas durante a gastrulação e origina o tubo digestivo primitivo e os orgãos a este associados. Durante o desenvolvimento, cada região do tudo digestivo primitivo é caracterizada por motivos de expressão distintos que determinam a localização exacta onde os diferentes orgãos deverão surgir ao longo do eixo antero-posterior. Ao mesmo tempo, o tubo digestivo primitivo também é especificado ao longo to eixo dorso-ventral, e a maioria dos orgãos surgem ventralmente. O mecanismo que leva à formação do eixo dorso-ventral no tubo digestivo primitivo é ainda mal compreendido. No tubo neural este processo foi extensivamente estudado e é descrito como um equilibro entre a expressão de Bone Morphogenetic Protein (BMP)4 - dorsalmente - e de Sonic Hedgehog (SHH) - ventralmente. Para além disso, diversos estudos indicam que sinalização pela BMP é necessária para a formação de alguns orgãos ventrais associados ao tubo digestivo primitivo. Tendo isto em conta, propomos que a via de sinalização da BMP poderá ser responsável por conferir identidade ventral ao tubo digestivo.

Neste projecto, caracterizamos um ratinho mutante previamente gerado pelo nosso grupo, em que *Cre*^{ERT2} é expressa sobre o controlo do promotor de *Sox17.* Este fator de transcrição é expresso na DE antes da formação do tubo digestivo primitivo. Após a caracterização, o ratinho foi utilizado para inativar condicionalmente a via de sinalização da BMP no tubo digestivo, através de inativação dos receptores principais da BMP. Os resultados preliminares estão geralmente de acordo com outros estudos que se focaram no papel da BMP na formação do tubo digestivo e orgão adjacentes. Para além disso, os resultados sugerem que a via de sinalização da BMP é essencial para a formação de orgãos ventrais como os pulmões e o primórdio pancreático ventral, algo que não foi previamente descrito.

Palavras chave: Endoderme definitiva, eixo dorso-ventral, BMP, Sox17

Abstract

The definitive endoderm (DE) is one of three germ layers segregated during gastrulation and it gives rise to the primitive gut tube and all associated organs. During development, each region of the primitive gut tube is characterized by unique expression patterns that determine the precise locations where organs emerge along the anterior-posterior axis. At the same time, the primitive gut is also patterned along the dorsal-ventral axis, with most organs emerging on the ventral side of the gut. Dorsal-ventral patterning is still poorly understood in the gut tube. In the neural tube, dorsal-ventral patterning is well described as a balance between expression of Bone Morphogenetic Protein (BMP)4 - dorsally - and Sonic Hedgehog (SHH) - ventrally. Furthermore, several distinct studies indicate that BMP is required in the formation of some of the ventral gut organs. Taking this into consideration, we theorized that BMP signalling could be a general cue providing ventral identity to the gut tube.

In this study, a mouse line previously generated by our group is characterized in which *Cre*^{ERT2} is expressed under the control of the promoter of *Sox17*. This transcription factor is expressed in definitive endoderm cells at a very early stage, previous to primitive gut formation. Thereafter, this mouse line is used as a tool in order to conditionally inactivate the BMP pathway in the DE, by knocking out its main receptors. Preliminary data are generally in accordance with previous observations made for the role of BMP in gut patterning and organ formation. Furthermore, we find BMP signalling to be essential for the formation of ventral organs like the lungs and the ventral pancreas, which had not been reported previously.

Key words: Definitive endoderm, Patterning, BMP, Sox17

Figure Index

Table Index

Glossary

AIP - Anterior Intestinal Portal

Alk - Activin-like kinase

Alk2 - Activin A receptor type I, or ACVRI

Alk3 - BMP receptor 1A, or BMPR1A

Alk6 - BMP receptor 1B or BMPR1B

AP - Anterior-Posterior

BMP - Bone Morphogenetic Protein

BMPR1A - BMP receptor 1A, or Alk3

BMPR1B - BMP receptor 1B, or Alk6

CIP - Caudal Intestinal Portal

DE - Definitive Endoderm

DV - Dorsal-Ventral

ExE - Extraembryonic Ectoderm

SHH - Sonic Hedgehog

SOX17 - Sex determining region Y box 17

VE - Visceral Endoderm

Chapter I

Introduction

Introduction

The ability to generate specific cell types that can develop into tissues or even functional organs holds the promise to treat a long array of health issues while eliminating some of the major problems currently associated with organ transplantation. Currently, engineered tissues are also being used to generate models for drug testing or for studying disease emergence and progression[6,7]. Organ formation is characterized by a vast intricacy in signalling pathways and architecture that is difficult to replicate. In order to efficiently recapitulate tissue and organ development *in vitro,* we must first understand how specific signalling pathways orchestrate organogenesis *in vivo*, by studying the developing embryo.

In this study, we aim at understanding the general principles that lead to the formation of different organs from the endoderm, focusing on the role of the BMP pathway.

1.1. Formation of the Primitive Gut Tube

The organism is derived from three primary germ layers. The ectoderm gives rise to the epidermis and the nervous system[8]; the mesoderm differentiates into connective tissues, the muscles, the vasculature and the hematopoietic system[9]; the definitive endoderm (DE), also called endoderm, forms the digestive tract and respiratory system, as well as their associated organs[5]. The three germ layers are specified during gastrulation, which starts at around 6 days and a half post-fertilization (E6.5) in mice. At this point, the embryo comprises a bilaminar cup-shaped epithelium where an outer visceral endoderm (VE) layer encapsulates the proximally positioned extraembryonic ectoderm (ExE), and the distally positioned epiblast that will go on to form the actual embryo (Figure 1.1).

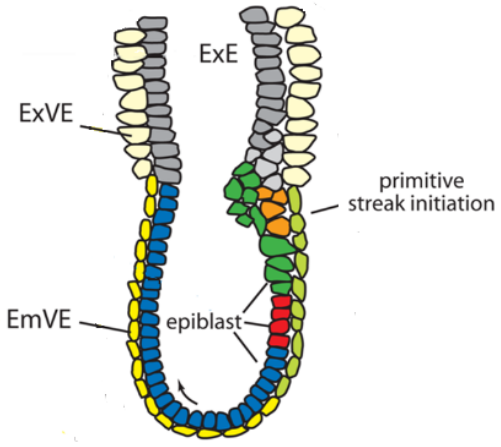

Figure 1.1. Gastrulating mouse embryo. The embryo is enveloped by the VE which is divided into extraembyonic (ExVE, white) and embryonic (EmVE, yellow and green). The ExVE gives rise to the yolk sac while the EmVE may take part in gut tube formation. The extraembryonic ectoderm (ExE, grey) locates proximally and the epiblast distally. The epiblast is constituted by prospective ectoderm (blue), mesoderm (red) and endoderm (green). The primitive streak locates in the posterior region of the epiblast. Orange - prechordal plate; Light grey - extraembryonic mesoderm.

Gastrulation starts when epiblast cells ingress locally in the posterior region of the epiblast - the primitive streak - emerging as nascent mesoderm. The newly formed mesenchymal layer locates between the inner epiblast cells and the outer visceral endoderm (VE). The last cell population to emerge from the primitive streak constitutes the DE (reviewed in Nowotschin and Hadjantonakis [10]). Early cell labelling studies, combined with molecular marker analysis indicated that DE cells displace the VE cells into the extraembryonic domain, where these form the yolk sac. However, recent studies suggest that some VE cells persist in the DE layer and even participate in primitive gut tube formation[11,12].

At the end of gastrulation, the DE constitutes a sheet of cells on the external surface of the mouse embryo. Over the next 24 hours embryonic tissues are rearranged forming the primitive gut tube, surrounded by the mesoderm. The movements involve the invagination of the DE in two different sites, one anterior at the anterior intestinal portal (AIP) and one posterior at the caudal intestinal portal (CIP) forming two dead end tubes which thereafter extend caudally and rostrally, respectively, meeting in the midgut region. During this process the cells on the lateral sides of the DE migrate toward the ventral midline of the gut tube while the medial part of the DE roughly forms the dorsal wall of the primitive gut tube. The closure of the primitive gut tube is associated with axial turning, which gives to the embryo its characteristic fetal shape (Figure 1.2).

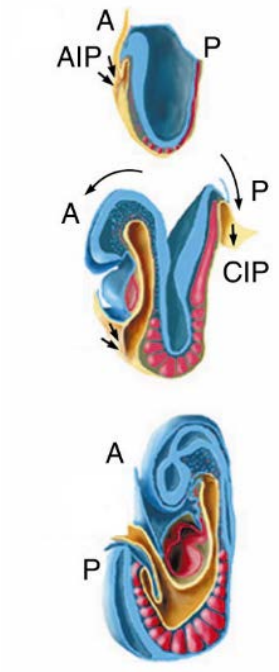

Figure 1.2. Gut tube closure and turning. Endodermal, mesodermal and ectodermal layers are respectively shown in yellow, red and blue. Mouse embryos (E8.0, 8.5 and 9.0) are pictured. In mouse, a crescent-shaped fold appears in the endoderm at the level of the tip of the neural tube and moves posteriorly (AIP) as indicated by arrows. A similar fold later arises at the very posterior end of the embryo and moves anteriorly (CIP). Convergence of these folds is facilitated by the turning of the embryo (big arrows). A - anterior; P - posterior; D - dorsal; V - ventral.

1.2. Patterning of the Primitive Gut Tube

While the gut tube is closing, regions of the gut are specified along the anterior-posterior (AP) axis into the different DE-derived organs. The rigorous organization pattern along the AP axis is orchestrated by reciprocal inductive signals between the endoderm and the surrounding mesoderm. Initially, broad domains can be identified by

expression of Hhex, Sox2, and Foxa2 transcription factors in the anterior half of the embryo opposed to the expression of Cdx1, Cdx2, and Cdx4 in the posterior half. These transcription factors are critical for regional foregut and hindgut identity, respectively. Already at this stage the two domains show distinct developmental potential and respond differently to subsequent signalling from the mesoderm. For example, graded levels of FGF signalling from the anterior foregut induce distinct fates. The highest levels induce the expression of Nkx2.1 in the future lung and thyroid progenitors, moderate doses activate liver progenitor fate, and lower levels promote the expression of Pdx1 specifying the pancreas and the duodenum. BMP activity is also present as a decreasing signal from the anterior side of the embryo. The effect of BMP signalling on gut patterning will be reviewed in the next sections. Eventually, these defined territories undergo morphogenesis, resulting in complex organs (reviewed in Zorn and Wells [5]).

The primitive gut tube is also patterned along the dorsal-ventral (DV) axis. Most organs emerge on the ventral side of the gut, with the exception of the dorsal pancreas and the parathyroids[13,14]. However, it is not known if general dorsalizing or ventralizing morphogens exist in mammals, although BMP4 has been shown to have a ventralizing effect in *Xenopus* animal cap[15].

1.3. BMP Signalling

BMPs were first identified for their capacity to induce ectopic bone formation[16]. Since then, they have been shown to be involved in pleiotropic morphogenetic processes (reviewed in Wagner, et al. [17]). Similarly to other members of the TGFβ superfamily, BMPs are large dimeric proteins synthesized and folded in the cytoplasm as inactive precursors. After being activated by proteolytic cleavage (*e.g.* Furin is required for BMP4 activity[18]), their functional C-terminal part is released into the extracellular compartment where it can signal to target cells by binding to receptor subunits Type I and Type II serine/threonine protein-kinase. Once the multimeric complex is formed, Type II receptors transphosphorylate Type I receptors which in turn phosphorylate the downstream receptor regulated R-Smad proteins - Smad1, Smad5, Smad8. Phosphorylated R-Smads associate with the co-mediator Smad4 and migrate to the nucleus, where they activate the expression of their target genes[19,20] (Figure 1.3).

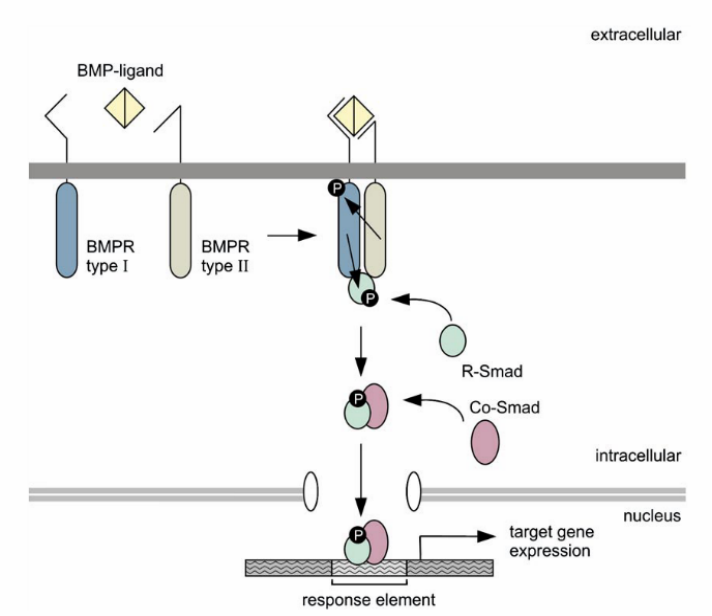

Figure 1.3. Cascade of BMP signalling. BMP dimers bind to serine/threonine kinase receptors type I and II. Upon ligand binding, type II receptors transphosphorylate type I receptors. The latter phosphorylate members of the Smad family of transcription factors. These Smads are subsequently translocated to the nucleus, where they activate transcription of target genes.

More than 30 ligands are able to activate BMP signalling. They are structurally related and can be further subdivided into subgroups. Two of them, *Bmp2* and *Bmp4,* diverged from a common ancestral gene and encode closely related proteins[21].

Bmp4 and *Bmp2* are both expressed in the extraembryonic tissues, although *Bmp2* expression is predominant. In the embryo, *Bmp2* is strongly expressed in the cardiac crescent at E7.25. Like *Bmp2*, *Bmp4* expression is observed in the heart but it is restricted to the inflow and outflow tracts. Both are expressed at E9.0 in the dorsal neural tube. During the gut tube closure at E7.25, *Bmp2* is strongly expressed in the closing anterior gut tube, while being notably absent from the open gut region. Thereafter, *Bmp2* is almost undetectable in the midgut and the foregut at the exception of the liver primordium at E9.0. On the contrary *Bmp4* is expressed in the thyroid primordium. At E10.5, Bmp4 is also strongly expressed in the lung bud mesenchyme and on the right dorsal side of the gut tube, along the stomach and pancreas[22].

Although both ligands show some functional redundancy, knocking out one or the other leads to different phenotypes. *Bmp4* null embryos phenotype is background dependant. The formation of the mesoderm may be severely impaired due a gastrulation defect and the embryos die at the start of gastrulation (E6.5), whereas other mouse strains survive until early organogenesis (E9.5)[23]. On the contrary, *Bmp2* knockout mice are able to gastrulate, they die at around E8.5 due to amnion/chorion or heart development defects[24].

1.4. Bmp receptors: Alk2, Alk3 and Alk6

The abundance of ligands in the BMP family is not matched by similar numbers of receptors. Thus the BMP pathway has highly promiscuous ligand-receptor interactions. Two Type I receptors - BMPR1A;ALK3 and BMPR1B;ALK6 - are known to translate signals from BMP2/4[21]. BMP4 has also been reported to bind to Type I A activin receptor ActR-I;ALK2 in the visceral endoderm (VE), although this pathway leads only to the activation of SMAD1/5 and not SMAD8[25]. This difference in the activation pattern of R-Smads by ALK3 and ALK6 or ALK2 is translated into distinct biological responses[26].

In contrast to the localized expression patterns of BMP ligands, expression of BMP receptors is widespread during early embryonic mouse development. *Alk3* and *BmpRII* are expressed in most tissues throughout development. *Alk6* expression starts later during development, after the gastrula stage. It is first observed at E7.5 in the AIP and is later expressed along the endoderm and in the liver primordium at E9.0. This expression pattern is maintained until E10.5, albeit at lower levels[22,27]. *Alk2* is expressed in pre-gastrulating and gastrulating embryos, mostly in extra-embryonic tissues (VE, chorion, amnion), and later, at E10.5, it is expressed in the head mesoderm as well as in the endocardium[28].

Mice lacking *Alk6* show only mild skeletal defects in the adult[29]. However, mouse embryos lacking *Bmp4*, *Alk3*, or *BmprII* are arrested at gastrulation, and mesoderm does not form[23,30,31].

1.5. BMP signalling in patterning of the gut tube

Very little is known about how the DE-derived organs acquire their positions along the DV axis in mammals. During organ specification when the DE still forms a sheet, the morphogens giving this information, if any, should first be positioned along the medio-lateral axis and after, the gut tub is closed, along the DV axis. Contrary to the endoderm, this process is well characterized in the ectoderm and seems to be a conserved system across vertebrates and insects, where antagonistic secreted factors determine first medial or lateral identity and later dorsal or ventral identity. For example, BMP4 orthologs found in fly and in vertebrates share similar functions and mechanisms for medio-lateral and later DV patterning in the ectoderm[32]. In mice, opposing gradients of sonic hedgehog (SHH) and bone morphogenetic protein (BMP) signalling are involved. BMP signalling is necessary to form laterally the non-neural ectoderm or surface ectoderm which becomes thereafter located dorsally in the neural tube. After

the neural tube is closed, the roof plate situated dorsally becomes a new organizing centre that produces BMPs which induce a dorsal fate in the interneurons present in the dorsal side of the neural tube (reviewed in Liu and Niswander [33]).

In the endoderm, several studies describe a role of BMP in the formation of some ventral organs all along the anterior-posterior axis (Figure 1.4). The thymus, which emerges on the ventral domain of the thymus-parathyroid primordium, is severely reduced when BMP signalling is inhibited by Noggin, an antagonist of BMP. Besides, it does not reach its final destination in the mediastinum[34]. Conversely, the presence of BMP4 in the dorsal domain where the parathyroid originates, reduces the expression of the parathyroid specific marker *Gcm2*[35]. BMP4 is necessary for the formation of the trachea in the ventral foregut [36]. The oesophagus does not form in absence of *Noggin*, a BMP antagonist. If BMP signalling is disrupted after lung specification, lung development is delayed and less branches are formed [37]In the absence of BMP4, the liver development is also delayed. In E9.5 mutant embryos, the hepatic epithelium did not yet bud contrary to their WT littermates [38]. Moreover, *in vitro* specification of hepatocytes from ESC-derived DE cells requires the presence of BMP4[39]. More globally, Xenopus ectodermal explants adopt a ventrolateral endodermal fate when *Bmp4* is overexpressed [15].

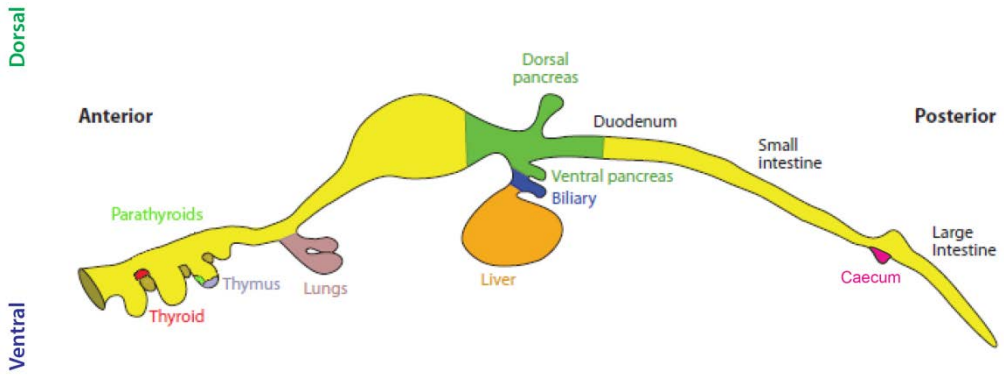

Figure 1.4. Primitive gut and associated organs. At E10.5 all organs associated to the gut tube have started to develop with a strict organization along the AP and DV axis.

These observations prompt the hypothesis that in mouse BMP signalling is a global cue that initially induces lateral identity to the DE and after gut tub closure, ventral identity forming a mirror-image of ectodermal and neural tube patterning. For the DE, BMPs secreted by the mesoderm would induce cell fate in the lateral regions of the DE which progressively join at the midline to form a tube. After gut closure, BMP

would act on the ventral side of the tube. Therefore, BMP signalling would be required for the ventral identity of the gut (Figure1.5).

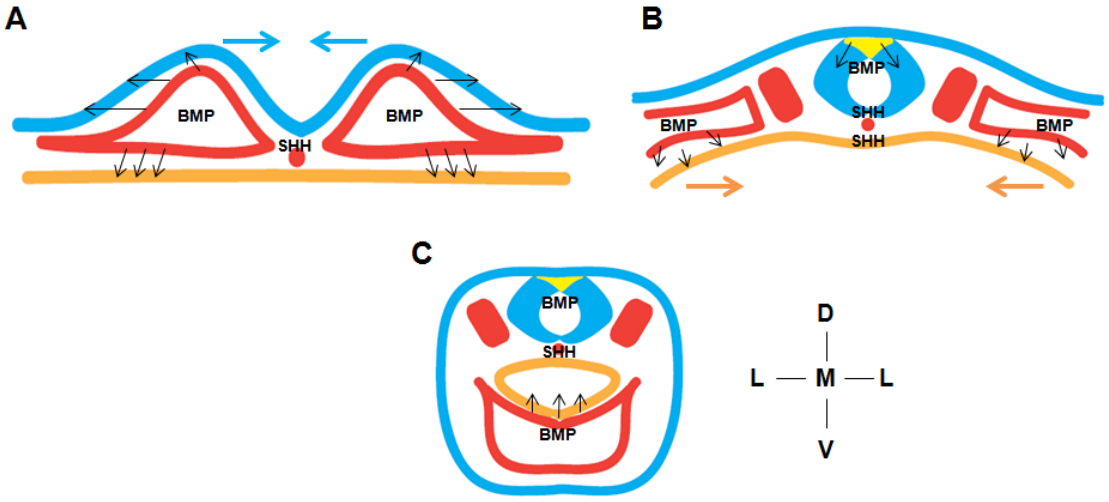

Figure 1.5. Mirror DV patterning in the neural tube and the gut tube. A. BMP is expressed in the lateral mesoderm (red) and secreted and patterns lateral ectoderm, while SHH secreted by the notochord (red dot) patterns medial ectoderm (blue). **B.** During the dorsal folding of the neural tube, the lateral ectoderm becomes the dorsal non-neural ectoderm (skin) and medial ectoderm forms the neural tube. In the neural tube, BMP starts being secreted in the roof plate (yellow) and patterns the dorsal region of the neural tube, opposed by SHH in the ventral region. We hypothesize that concurrently, BMP secreted in the mesoderm patterns lateral DE (orange) while SHH secreted in the notochord may pattern medial DE. **C.** The gut tube folds in a mirror image to the neural tube and thus lateral tissues end-up ventrally in the tube. After ventral closure, SHH secreted by the notochord may pattern the dorsal region of the primitive gut tube and BMP secreted in the mesoderm may pattern the ventral region. BMP secretion may form a medio-lateral and later dorsal-ventral gradient. Black arrows - BMP signalling; Blue arrows - neural tube closure; Orange arrows - gut tube closure. D - Dorsal; V - Ventral; M - Medial; L - Lateral.

However, the requirement of BMP signalling during gastrulation precludes further study during endoderm patterning. In order to explore the role of BMP in DV patterning of the gut tube, a time and tissue specific inactivation of the pathway is necessary. For example, in the respiratory tract, conditional inactivation of the BMP pathway was previously achieved by inactivating its two well characterized receptors - Alk3 and Alk6 in the future lung epithelium after organ specification[37]. Our aim was to inactivate it in the endoderm.

1.6. Sox17 Expression

The SRY (sex determing region Y)-box 17 (SOX17) is a transcription factor belonging to the Sox protein family. Sox proteins share similar DNA binding properties,

however individual Sox proteins appear to regulate specific sets of target genes *in vivo* due to restricted patterns of expression and in combination with specific cofactors interactions. Sox proteins are key players in the regulation of embryonic development and determination of cell fate (reviewed in Lefebvre, et al. [40]).

SOX17 is first expressed at the blastocyst stage between E3.25 and E4.5, in a salt and pepper pattern, where it promotes the primitive endoderm cell fate over the epiblast fate[41]. Subsequently, it is also expressed in the visceral endoderm around E6.0-E6.5 [42]. SOX17 is dynamically expressed in the DE, forming a temporal and spatial wave of expression from the anterior to the posterior region of this tissue. At first, expression is detected in the anterior end of the primitive streak at E7.0, which coincides with the time of ingression of future anterior DE cells. By E8.0 SOX17 is observed in the prospective posterior gut, while its expression in the foregut is already reduced. Its expression in the hindgut shuts down around E9.0. SOX17 is a key player in the definitive endoderm development as it is necessary for its specification[42,43]. After E9.0, SOX17 expression is observed in the hemogenic endothelial cells (ECs), which are of mesodermal origin[44]. SOX17 is then necessary for definitive hematopoiesis and the maintenance of the hematopoietic stem cell pool, both at the fetal and neonatal stages[1,45]. Notably, at around E9.5, SOX17 is again expressed in the ventrolateral region of the most posterior foregut, where the bile duct and gall bladder originate, and persists until at least E15.5[46]. Based on this expression pattern, it appears that Sox17 may be used as a driver to target gene inactivation widely in endoderm.

1.7. The Cre Recombinase System

Cre (cyclization recombination) gene encodes a site-specific DNA recombinase of the bacteriophage P1 which is required for the circularisation of the phage DNA - a critical step in the bacteriophage life-cycle. The enzyme recognizes a specific sequence of 34-bp, termed loxP, and catalyses both intra and intermolecular recombination between two loxP sites. Cre–loxP mediated recombination between two directly repeated loxP sites excises all DNA sequences located within the two sites as a covalently bound circular molecule[47].

The conditional deletion of a gene in mice (conditional knock-out) is achieved by excising with a Cre the gene flanked by two LoxP sites, also called floxed gene. The gene promoter driving Cre expression determines tissue or stage specificity. Temporal control of the onset of the mutation can be further achieved by using a Cre fused to a modified Estrogen Receptor (ERT2). Cre^{ERT2} is sequestered in the cytoplasm unless

tamoxifen, an estrogen analogue, is present and has been metabolically activated in the liver[48].

Sox17 promoter has already been used to drive the expression of Cre recombinase in the endoderm and in the hemogenic endothelial cells[1,49]. As it is specifically expressed in the DE cells at a particular stage of development, it is possible to target these cells using a CreERT2 system. This strategy has already been confirmed by generating a *Sox17*^{CreERT2} mouse line[50].

Another *Sox17*^{CreERT2} line has contemporarily been developed in our laboratory. The Cre recombinase fused to an estrogen receptor has been targeted to the Sox17 locus disrupting the gene after the second exon, in contrast to the previously published line (Figure 1.6) (Marine Rentler-Courdier-Kraus, unpublished data).

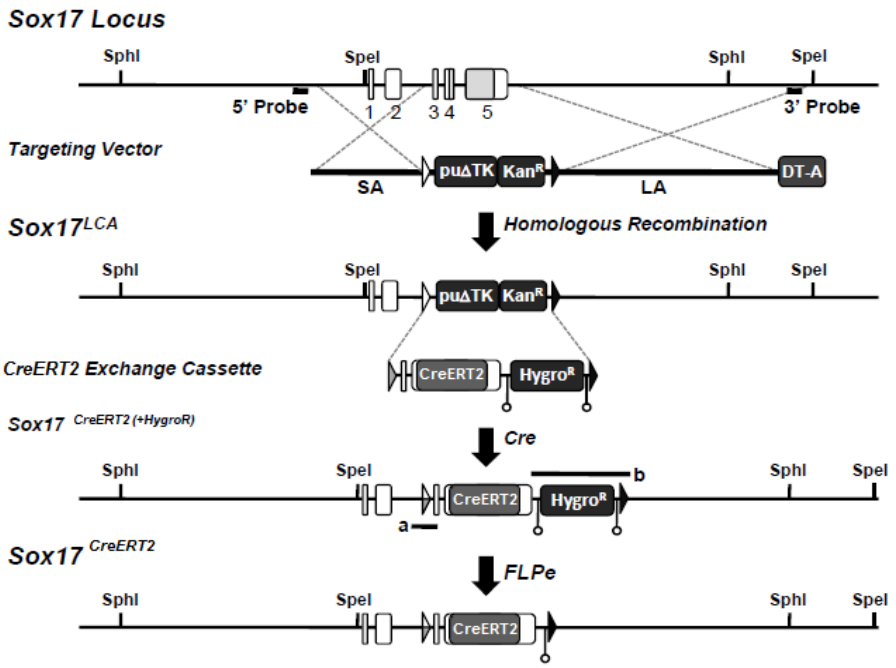

Figure 1.6. Diagram of the Sox17 locus, targeting vector, Sox17LCA allele, CreERT2 exchange cassette, Sox17GFPCre(þHygroR), and Sox17CreERT2 allele. A targeting vector for the mouse Sox17 gene was constructed where the sequence including exons 3–5, which contains the coding region of Sox17, was replaced with a puromycin resistance-D-thymidine kinase fusion gene (puDTK) and an EM7-driven kanamycin resistance gene (KanR) flanked by lox66 (open triangle) and lox2272 (black triangle) sites. The GFPCre exchange cassette was flanked by lox71 (gray triangle) and lox2272 sites and contained a phosphoglycerol kinase-driven hygromycin resistance gene (HygroR) flanked by flippase recognition target sites (open circles). This prepares the locus to easy replacement by any insertion and was previously used to insert a CreGFP fusion[1]. Following exchange into Sox17LCA-containing mouse embryonic stem cells by recombinase-mediated cassette exchange (RMCE), mice containing the Sox17CreERT2-(þHygroR) allele, were bred with FLPe-expressing transgenic mice, thereby generating the final Sox17CreERT2 allele. Abbreviations: DT-A, Diphtheria toxin A; LA, long arm; LCA, loxed cassette acceptor; SA, short arm.

1.8. General Aims and Strategy

Prior evidence suggests a role of the BMP pathway in the formation of several ventral endodermal organs. We hypothesised that BMP signalling acts as global ventralizing factor in the gut, mirroring its action in the neural tube where it is necessary for dorsal identity (Figure 1.3).

In the present study, we characterized the Sox17Cre^{ERT2} mouse line that was previously generated in our lab in order to determine the most reliable way to induce recombination in the DE without affecting the other tissues.

The newly characterized mouse line was then used to inactivate the BMP signalling pathway in the DE by deleting *Alk3* using the *Sox17^{CreERT2}*, in an *Alk6* null background. The outcome of the inactivation has been thoroughly analysed by whole mount imaging. For this purpose, efficient labelling of dorsal and ventral endoderm organ primordia was established.

Chapter II

Materials and Methods

Materials and Methods

2.1. Mouse breeding and genotyping

The Sox17^{CreERT2} allele was maintained within an ICR background for experiments. Mice with the Rosa26^{YFP}, Alk3^{flox} or Alk6^{-} allele were previously described[29,30,51] . The mating scheme used in order to obtain BMP pathway mutants is described in Table 2.1, along with the ratios of each genotype obtained in the progeny and the designations attributed for simplicity. Mice were housed at the University of Copenhagen. The Dyreforsøgstilsynet approved the mouse housing and experiments.

Midnight before a vaginal plug was observed was considered as the time of fertilization (E0). Pregnant females received an intraperitoneal injection of warmed tamoxifen (Sigma) dissolved in corn oil at a concentration of 10mg/mL, with a 25 gauge needle. Each female was weighed before injection and the volume of injected tamoxifen was calculated accordingly. To collect the embryos at the different time points (E9.5, E10.5, E12.5), the females were euthanized by cervical dislocation and the embryos were dissected out of the uterus in PBS. A part of the yolk sac was removed and used for genotyping. The embryos were fixed in PFA 4% (Sigma) for 2 hours on ice with shaking.

Table 2.1. Breeding scheme for BMP mutants

Parent 2 Alleles	**Parent 1 Alleles**	
	Alk3fl Alk6 + Sox17 +	Alk3fl Alk6 - Sox17 +
Alk3fl Alk6+ Sox17CreERT2	Alk3fl/fl Alk6+/+ Sox17CreERT2/+ 1/8 **Alk3 KO**	Alk3fl/fl Alk6+/- Sox17CreERT2/+ 1/4 **Hz**
Alk3fl Alk6- Sox17CreERT2	Alk3fl/fl Alk6+/- Sox17CreERT2/+ 1/4 **Hz**	Alk3fl/fl Alk6-/- Sox17CreERT2/+ 1/8 **dKO**
Alk3fl Alk6+ Sox17+	Alk3fl/fl Alk6+/+ Sox17+/+ 1/8 **WT**	Alk3fl/fl Alk6+/- Sox17+/+ 1/4 **Alk6 +/-**
Alk3fl Alk6- Sox17+	Alk3fl/fl Alk6+/- Sox17+/+ 1/4 **Alk6 +/-**	Alk3fl/fl Alk6-/- Sox17+/+ 1/8 **Alk6 KO**

PCR genotyping was performed on tail tip genomic DNA and embryonic tissue after lysis in 100µL PCR direct tail buffer (Viagen) containing 2,5µL 20,6 mg/mL Proteinase K (Roche) overnight at 55ºC, followed by Proteinase K heat inactivation for 45 min at 85ºC. Each PCR reaction contained 2 to 4 µL of genomic DNA digestion solution, 5 µL of 5x Green GoTaq buffer (Promega), 1 µL of 5mM dNTPs (Thermo Fisher Scientific), 1 µL of 10 µM primer stock (Table 2.1), 0,2 µL of 5u/µL GoTaq enzyme (Promega) and miliQ to a final volume of 25 µL. All primers were ordered from Integrated DNA Technologies.

Table 2.2 Genotyping Primers

Locus	Primers	Annealing temperature Cº	product size	
			WT	mutant
Sox17	5'-TGCCAC GACCAAGTGACAGC-3' 5'-CCAGGTTACGATAT AGTTCATG-3'	58	no product	700
Rosa26	5'- AAAGTCGCTCTGAGTTGTTAT-3 5'-GCGAAGAGTTTGTCC TCAACC-3' 5'-GGAGCGGG AGAAATGGATATG-3'	58	600	300
Alk3	5'-GCAGCTG CTGCTGCAGCCTCC -3' 5'-TGGCTACAATTTGTCT CATGC-3'	50	350	600
Alk6	5'-CCCAAGATCCTACGT TGTAA-3' 5'-GAGTGGTTACAACAAGATC AGC A-3' 5'-GCCCTGAATG AACTGCA GG-3'	62	150	230

Electrophoresis gels were prepared with 2% ultra pure agarose (Thermo Fisher Sci.) in TAE 1x (in house) containing 0,003% ethidium bromide (Thermo Fisher Sci.). In each well, 6 µL of the PCR reaction was loaded as well as a 1kb DNA ladder (Thermofisher Scientific). The gels were submitted to 80mV voltage on a standard power pack p25 (Biometra) for roughly 20 min and imaged with a molecular imager (GelDoc XR+, BioRad).

2.2. Immunofluorescence

2.2.1. Immunofluorescence on sections - General protocol

Fixed embryos were thoroughly washed with PBS (1.8 mM KH_2PO_4, 10 mM Na_2HPO_4, 137 mM NaCl, 2.7 mM KCl pH7.4)[a] and incubated in a solution of 0.12M

[a] Steps where the temperature is not mentioned were performed at room temperature.

phosphate buffer 15% sucrose (Merck) (sucrose) overnight at 4ºC for cryoprotection. Fresh sucrose solution was added for 30 min, followed by 0.12M phosphate buffer 15% sucrose 7.5% gelatin (Sigma) (gelatin) at 38ºC for 30 min. The embryos were embeded in a gelatin block and the block set at 4ºC for 15 min. The gelatin blocks were then unmolded. They were frozen at -65ºC for 1 min. The blocks were stored at -80ºC until use. Sections of 7µm thickness were obtained using a cryostat (CM1959 Leica) at -24ºC. The cryosections were stored at -20ºC on Superfrost Plus Slides slides (ThermoFisher). The general protocol forimmunofluorescence on sections consisted of a drying step of 5 min , followed by rehydration with tris buffer (50 mM Tris pH 7.5, 150 mM NaCl) 0,01% triton (TBST), permeabilization with tris buffer 0,25% triton (Applichem), washing with TBST 3x5 min and blocking with 10% donkey serum (Sigma) in TBST for 1 hour. All primary antibodies (see Table 2.1) were diluted in blocking solution and the sections covered by the antibody solution were incubated overnight at 4ºC. The sections were then washed with TBST 3x15 min and the respective secondary antibodies (See table 2.2) were diluted in blocking solution and centrifuged for 10 min at 21000 rcf, at 4ºC. Secondary antibodies and DAPI (Sigma) were incubated for an hour, after which the slides were again washed with TBST 3x15 min. The slides were mounted with 50% glycerol (Sigma) solution in PBS and kept at 4ºC until imaging. All images were acquired with either a wide field (DM5500B, Leica) or a confocal (LSM 780, Zeiss) microscope.

2.2.2. Antigen Retrieval

In some cases, antigen retrieval was performed after the washes following the permeabilization steps. The slides were equilibrated for 5 min in 10mM trisodium citrate buffer pH6 and warmed gradually from 65ºC to 95ºC in an automated epitope recovery device (PT module, Lab vision). This temperature was maintained for 20 min after which it went down to 65ºC.The slides were then washed 3x5 min with TBST and the rest of the immunofluorescence was carried out as usual.

2.2.3. Antibody Stripping

Antibody stripping was performed in order to allow sequential staining with two antibodies derived from the same species. After the first immunofluorescence, the sections were washed in TBST and incubated for 1 hour at 60 ºC in a solution of 62,5 mM Tris-HCl (Sigma), 2% SDS (Sigma) and 0,8% β-mercaptoethanol (Sigma)[52]. The

slides were then washed extensively in running tap water for 10 min, rinsed in 95% ethanol (Merck) followed by milliQ water and by TBST. The general protocol was continued from this step on. When Tyramide Signal Amplification kit (Thermo Fisher Sci.) is used in the first round of staining, both antibody stainings can be imaged at the same time.

1.2.4. Phosphatase Assay

In order to ensure specificity of the pSMAD1/5/8 antibody to the phosphorylated form of this protein a phosphatase assay was performed. After permeabilization and washes in TBST, the sections were washed 2x2 min in milliQ water and rinsed in TBST. Each slide was treated with a solution of Lambda Phosphatase (New England Biolabs) prepared according to the manufacturer's instructions, for 2 hours at 37ºC. After the treatment, the slides were washed 2x5 min in milliQ water followed by 5 min in TBST. The general protocol was carried on from this point.

1.2.5. Wholemount Immunofluorescence

Fixed embryos were thoroughly washed with PBS and gradually dehydrated to Methanol (Sigma) with sequential dilutions (50%Methanol in PBS, 100%Methanol in PBS) for at least 15 min each. These embryos were stored at -20ºC.

The embryos were incubated in a solution of 16% DMSO (Sigma) and 5% H_2O_2 (Sigma) in methanol overnight at 4ºC. The samples were rehydrated to PBST. Blocking solution - PBS 0,5% Tween (Sigma) (PBST) containing 1%BSA (Roche) - was added and incubated for 8 hours or overnight. Primary antibodies were diluted in blocking solution and incubated for 40 to 48 hours at 4ºC. Primary antibodies were washed with PBST extensively all day or overnight at 4ºC and secondary antibodies were added diluted in blocking solution and incubated for 40 to 48 hours at 4ºC. Secondary antibodies were washed with PBST extensively all day or overnight at 4ºC and finally the samples were gradually dehydrated to methanol with sequential solutions (Methanol 50%, 100%) for at least 15 min each. All steps of the protocol were carried out over mild agitation using a rocking platform. These samples were stored at -20ºC until imaging. Before imaging by confocal microscopy, samples were cleared in 33% Benzyl Alcohol (Merck) 66% Benzyl Benzoate (Merck) (BABB) overnight and mounted in depression slides. All wholemount immunofluorescence samples were scanned on a confocal (SP8, Leica) microscope. After imaging, samples were again stored in

methanol at -20ºC, until further experiments. All image processing and analysis was performed on Imaris 8.1 software.

Table 2.3. Primary Antibodies

Targeted antigen	Origin	Sections	Wholemount	Supplier
CD31	rat	1/50	n.a[a]	550274 Becton Dickinson
E-CAD	rat	1/200	n.a	U3254 Sigma
GCM2	rabbit	1/200	1/500	ab64723 Abcam
GFP	chick	1/1000	1/1000	ab13970 Abcam
HLXB9	rabbit	1/1000[b]	1/1500	ab26128 abcam
INS	guinea pig	1/200	n.a	A0564 Dako
NKX2.1	mouse	1/200	1/500	PA0100 Biopat Im.
PITX2	rabbit	1/500	1/1000	PA1020 Capra Science
PROX1	goat	n.a	1/500	homemade[c]
PROX1	rabbit	1/100	n.a	AF2727 R&D Systems
pSMAD1/5/8	rabbit	1/200	n.a	9511 Cell Signaling
SOX2	rabbit	1/200	n.a	AB5603 Chemicon

Table 2.4. Secondary Antibodies

Against	Origin	Conjugated	Sections and wholemount	Supplier
chick	donkey	Al488	1/800	Thermo Fisher Sci.
goat	donkey	Al568	1/1000	Thermo Fisher Sci.
goat	donkey	Al488	1/1000	Thermo Fisher Sci.
guinea pig	goat	Al568	1/800	Thermo Fisher Sci.
mouse	donkey	Al568	1/1000	Jackson IR
mouse	donkey	Al488	1/1000	Thermo Fisher Sci.
rabbit	donkey	HRP[d]	1/100	Jackson IR
rabbit	donkey	Al488	1/200	Jackson IR
rat	donkey	Al647	1/500	Jackson IR

[a] n.a. non applicable
[b] Antigen recovery was performed in this case
[c] Gift from Tatiana Petrova
[d] Tyramide Signal Amplification kit used for detection

Chapter III

Results and Discussion

Results and discussion

3.1. Characterization of the new Sox17CreERT2 line

A Sox17Cre^{ERT2} mouse was previously generated in our lab by Marine Rentler-Courdier. In order to generate the Sox17Cre^{ERT2} ES cell line, the coding sequence of a Cre^{ERT2} fusion protein was targeted after the second exon of Sox17 disrupting the gene. From this ES cell line, a mouse line was generated (unpublished data). The main difference between this mouse strain and the one reported by Engert (2013) is that the *Sox17* gene is disrupted in the mutant allele.

Sox17 is expressed transiently in different tissues. Recombination will therefore occur in the cells that are expressing Sox17 if the activated form of tamoxifen is present as it is required for the translocation of the Cre^{ERT2} to the nucleus. In order to evaluate tamoxifen induced cell recombination in this new CreERT2 line, heterozygous mice were crossed with the *Rosa26$^{YFP/YFP}$* (*R26*) Cre reporter mice[51]. In their progeny, *yellow fluorescent protein* (*YFP*) is expressed after Cre-mediated excision of the *loxP*-flanked stop cassette from the ubiquitously expressed *Rosa26* locus, allowing the detection of the recombined cells. Different injection time points with variable doses were investigated in order to reach the maximum recombination efficiency in the DE with little effect on the vasculature and the yolk sac.

We initially chose to activate Cre by tamoxifen injection at E7.5 (Figure 3.1), when expression of *Sox17* is mostly restricted to the DE[42,53]. In order to get a homogenous recombination rate among litters, the dose of injected tamoxifen is function of the weight of the pregnant female and expressed as the amount of tamoxifen per 10g of mice (mg/10g).

Another critical point was the age of the tamoxifen solution. Indeed, oil solubilized tamoxifen is unstable. However, its degradation also coincides with a reduced toxicity. Indeed, it was possible to harvest E12.5 embryos which received 0.7mg/10g of tamoxifen at E7.5 with a tamoxifen solution was older than 3 months (n=1). With this setting, most of the cells in the gut endoderm as well as in the endoderm derived organs expressed YFP (Figure 3.1 - A-C). Concomitantly, no recombined cells were found in the yolk sac epithelium (Figure 3.1 - D) and only few in the vasculature (Figure 3.1 - E - white arrow), indicating that at the time of injection *Sox17* expression was almost limited to the DE, with only few cells of mesodermal origin being *Sox17*$^{+}$..

On the contrary, when attempting to repeat the experiment, it was observed that injection of the same dose of freshly prepared tamoxifen was lethal (n>5). Since it

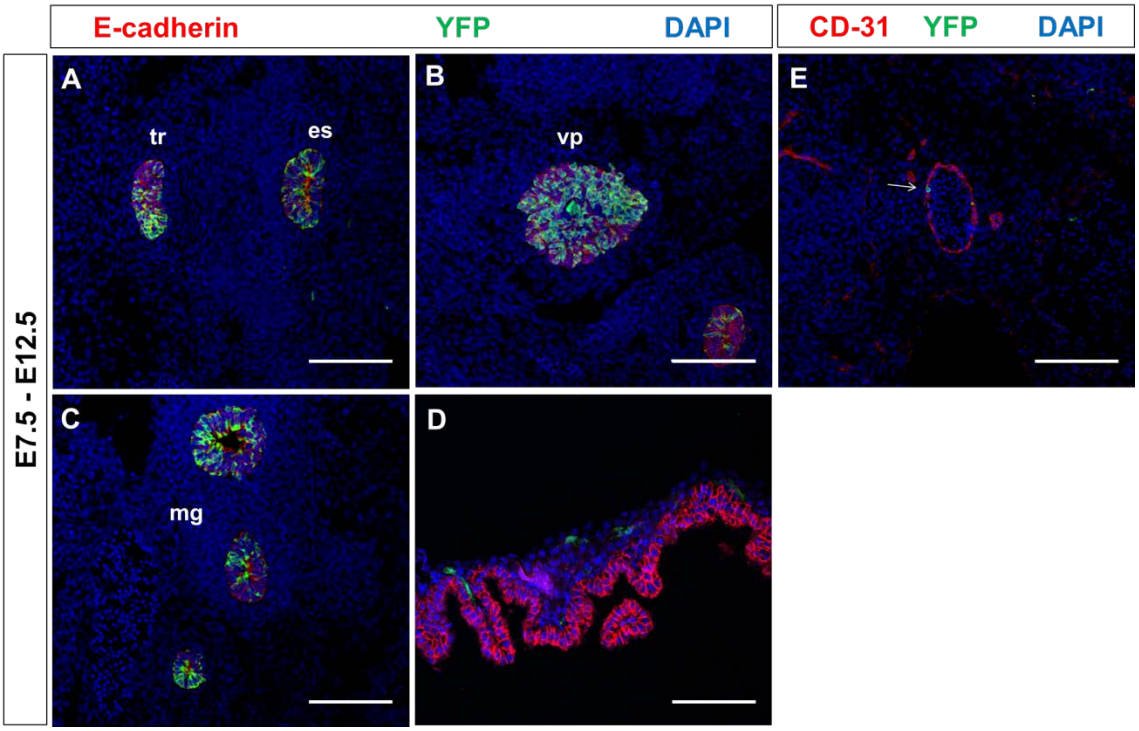

Figure 3.1. Recombination rates in E12.5 embryos after administration of out of date tamoxifen at E7.5. (A-D) Immunofluorescence for E-Cadherin and GFP on sections of *Sox17*$^{CreERT2/+}$ *Rosa*$^{YFP/+}$ E12.5 embryos shows the recombination when old tamoxifen is injected at E7.5. Around 70 to 90% of the gut endoderm highlighted by E Cadherin (red) were recombined and expressed YFP detected by the GFP antibody as exemplified in the trachea and esophagus (A), the pancreas (B) and the midgut (C). Only few GFP positive cells were observed in the yolk sac epithelium (red) (D). (E) Immunofluorescence for CD31 and GFP on sections of *Sox17*$^{CreERT2/+}$ *Rosa*$^{YFP/+}$ E12.5 embryos shows rare event of recombination in the endothelial cells expressing CD31 (red) when old tamoxifen is injected at E7.5. Nuclei are counterstained with DAPI (blue). Abbreviations: es - esophagus; tr - trachea; vp - ventral pancreas; mg - midgut. Scale bar - 100 µm.

cannot be excluded that the outcome on the recombination will be more variable due to the partial tamoxifen degradation, further injections were performed with fresh tamoxifen, solubilized less than three days-old prior to injection. Nevertheless, the previous experiment showed that the time window of injection targeted mostly DE cells.

Since tamoxifen injection of 0.7mg/10g was lethal for the litter, most probably due to cardiac developmental defects, lower doses of tamoxifen were used. A tamoxifen injection of 0.6mg/10g was found to be the highest dose administered at E7.5 that does not cause high rates of developmental delay and malformation followed by abortion. At E9.5 the number of recombined cells was variable across different litters, and never higher than 30% when 0.6mg/10g or 0.5mg/10 were injected (n=5 combining 0.5mg/10g and 0.6mg/10g) (Figure 3.2). The recombination variability may be caused by the lower dose of tamoxifen as a critical amount is necessary for Cre

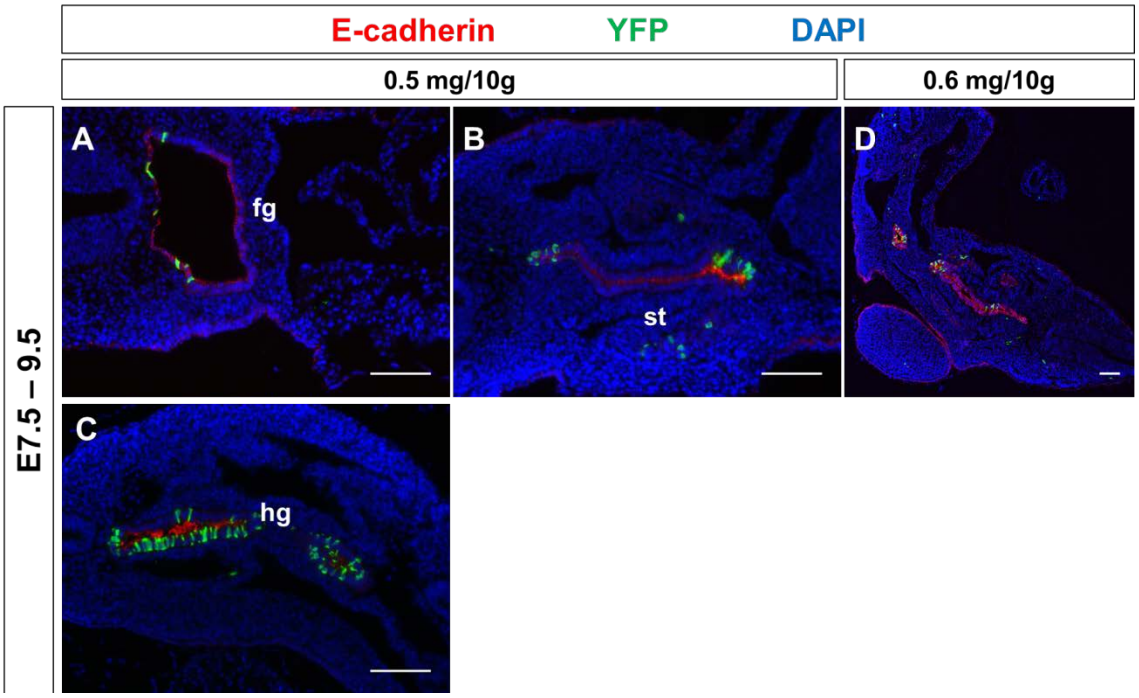

Figure 3.2. **Recombination rates in E9.5 embryos after administration of tamoxifen at E7.5.** (A-C) Immunofluorescence for E-Cadherin and GFP on sections of *Sox17*$^{CreERT2/+}$ *Rosa*$^{YFP/+}$ E9.5 embryos shows the recombination when tamoxifen is injected at E7.5 with a dose of 0,5 mg/10g or (D) a dose of 0,6 mg/10g. Few cells of the gut endoderm highlighted by E Cadherin (red) were recombined and expressed YFP detected by the GFP antibody. Often, more cells were recombined in the posterior region gut as exemplified in the hindgut compared to the foregut (A and C). Nuclei are counterstained with DAPI (blue). Abbreviations: es - esophagus; tr - trachea; vp - ventral pancreas; mg - midgut. Scale bars - 100 um.

activation and by the dynamic expression of Sox17. But also, considering the rapid shift in *Sox17* expression, it is likely that even small discrepancies in the time of tamoxifen injection will result in the recombination of different groups of cells. Sox17 expression is first found in the prospective foregut (E7.0) and gradually shifted until it is only found in the prospective hindgut (E9.0)[42]. In line with the dynamic expression pattern, it was observed that often more cells were recombined in the posterior region of the gut than in the foregut (Figure 3.2 A-C), which indicates that the DE cells of the foregut were no longer Sox17^{+} at the time of Cre activation.

According to the previous experiment, an earlier injection than E7.5 would be needed in order to induce recombination in the prospective foregut cells. Preliminary experiments in the lab have shown that injection of 0.7mg/10g at E6.5 leads to high recombination rate (around 90%) in the whole gut at E9.5 but results in embryonic lethality since no embryo survived after E10.5 (unpublished data). It is noteworthy that the tamoxifen solution used for this experiment was not fresh. Therefore, a strategy

combining lower doses of tamoxifen (0.4mg/10g) injected at two different time points was undertaken in order to improve the recombination in Sox17^{+} DE cells and the viability of the embryos. Using this approach, we observed that between 70 to 90% of the cells in the gut endoderm were recombined both at E9.5 (n=2) and E12.5 (n=4). For example, most of the cells in the liver primordium were recombined at E9.5 (Figure 3.3 - B) and high recombination rates in the pancreas were observed at E12.5 (Figure 3.3 - E). The recombination in the vasculature might be caused by the presence of tamoxifen metabolites long after injection. The precise length of time that tamoxifen continues to induce recombination is highly variable depending on the dose and mode of administration[54,55]. Nevertheless, the low rates of recombination observed in the vasculature (~1%) in this experiment would be unlikely to interfere when analysing DE

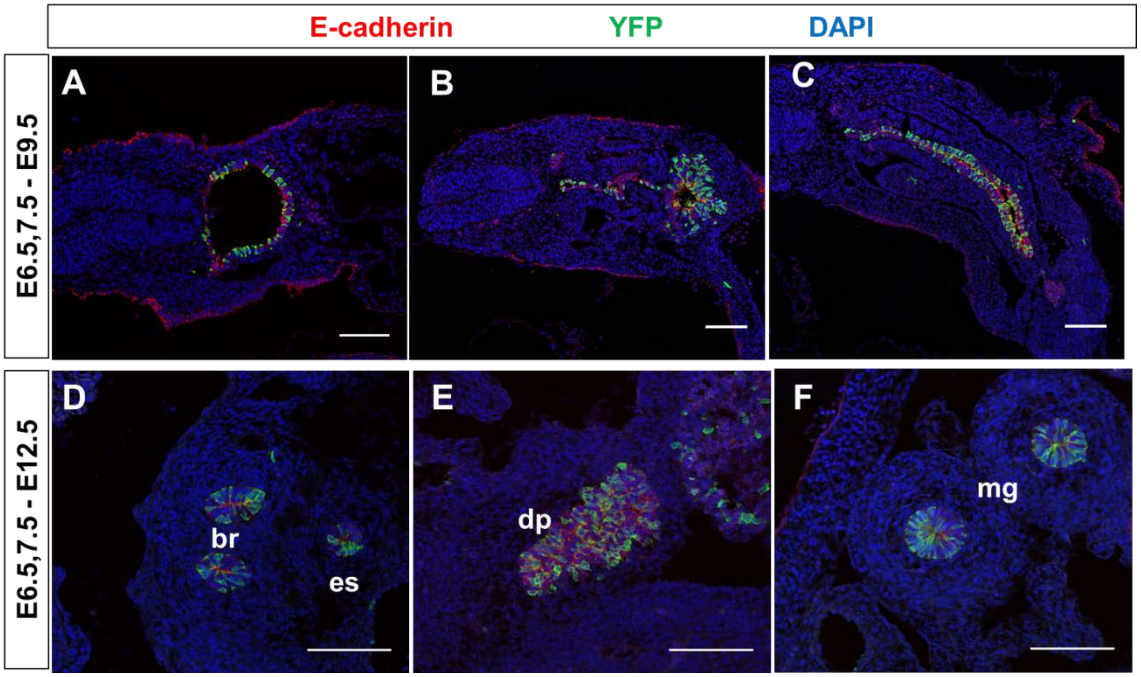

Figure 3.3. Recombination rates in E9.5 and E12.5 embryos after administration of tamoxifen twice, at E6.5 and E7.5. (A-C) Immunofluorescence for E-Cadherin and GFP on sections of *Sox17*$^{CreERT2/+}$ *Rosa*$^{YFP/+}$ E9.5 embryos shows the recombination when tamoxifen is injected at E6.5 and E7.5 with a dose of 0,4mg/10g/day. Around 70 to 90% of the gut endoderm cells highlighted by E Cadherin (red) were recombined and expressed YFP detected by the GFP antibody as exemplified in the foregut (A), the liver primordium (B) and the hindgut (C). (D-F) Immunofluorescence for E-Cadherin and GFP on sections of *Sox17*$^{CreERT2/+}$ *Rosa*$^{YFP/+}$ E12.5 embryos shows the recombination when tamoxifen is injected at E6.5 and E7.5 with a dose of 0,4mg/10g/day. Around 70 to 90% of the gut endoderm highlighted by E Cadherin (red) were recombined and expressed YFP detected by the GFP antibody as exemplified in the esophagus and main bronchi (D), dorsal pancreas (E) and the midgut (F). Nuclei are counterstained with DAPI (blue). Abbreviations: br - bronchi; es - esophagus; dp - dorsal pancreas; mg - midgut. Scale bars - 100 µm.

lineage-restricted conditional mutants. This double injection strategy was found to be the most effective and reliable way to induce DE specific Cre activity with this new *Sox17*^{CreERT2} line.

After E9.0, *Sox17* expression is found on a subset of endothelial cells of the blood vessels, including the dorsal aorta[45]. When *Sox17* is no longer expressed in the DE, it is re-expressed in the ventrolateral region of the most posterior foregut, where the bile duct and gall bladder originate[46]. In order to verify the ability of the *Sox17*^{CreERT2} line to recombine cells in these tissues, 0.7mg/10g of tamoxifen were administered at E10.5 and the embryos harvested at E14.5 (n=2), when the organs and vasculature are mainly formed. We observed that many endothelial cells in the vasculature were recombined, *e.g* in the dorsal aorta (Figure 3.4 - A-C). Furthermore, recombined cells were found in the bile duct, in accordance with *Sox17* expression (Figure 3.4 - D-F).

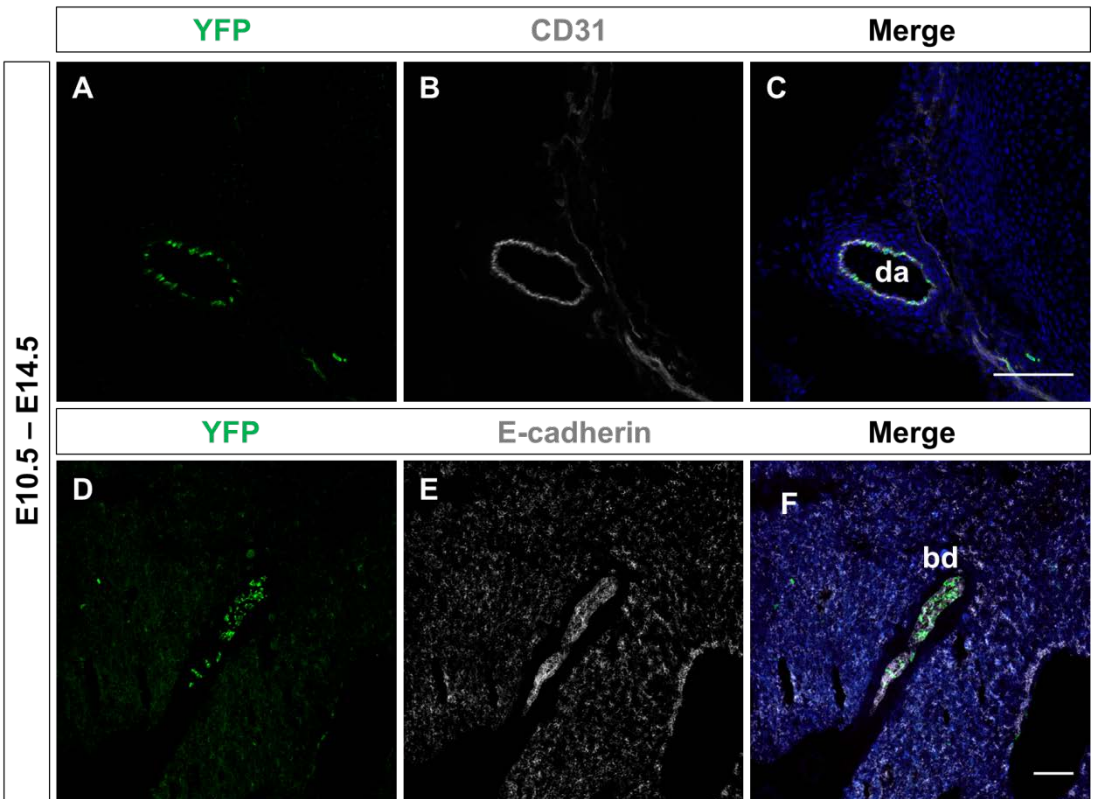

Figure 3.4. Recombination rates in E14.5 embryos after administration of tamoxifen at E10.5. (A-C) Immunofluorescence for GFP (green, single channel image (A)) and CD31 (gray, single channel image (B)) on sections of *Sox17*$^{CreERT2/+}$ *Rosa*$^{YFP/+}$ E14.5 embryos shows the recombination when tamoxifen is injected at E10.5. Very high numbers of recombined cells were observed in the vasculature. (D-F) Immunofluorescence for GFP (green, single channel image (D)) and E-Cadherin (gray, single channel image (E)) on sections of *Sox17*$^{CreERT2/+}$ *Rosa*$^{YFP/+}$ E14.5 embryos shows the recombination when tamoxifen is injected at E10.5. Very high numbers of recombined cells were observed in the bile duct.. Nuclei are counterstained with DAPI (blue). Abbreviations: da - dorsal aorta; bd - dile duct. Scale bars - 100 µm.

It has been shown that *Sox17* is still expressed at E9.0 in the ventral pancreas[50]. However, none of the pancreatic cells expressed YFP indicating that by E10.5, *Sox17* is no longer expressed in this organ (Figure 3.5).

After birth, SOX17 is essential for the regulation of insulin secretion in beta-cells. Mice lacking *Sox17* during pancreas organogenesis are more susceptible to develop diabetes[56]. Although no mature beta cells are present at E10.5[57], there are some cells co-expressing insulin and glucagon. They were not GFP positive at E14.5 indicating that neither the progenitors of beta cells nor the glucagon/insulin double-positive cells express *Sox17* at E10.5 (Figure3.5).

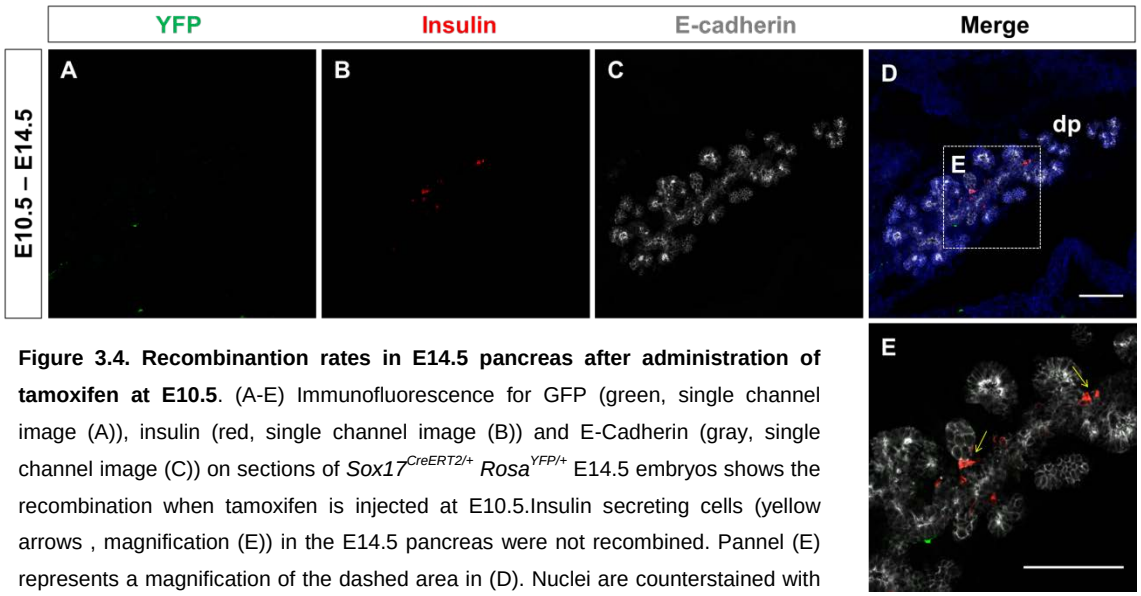

Figure 3.4. Recombinantion rates in E14.5 pancreas after administration of tamoxifen at E10.5. (A-E) Immunofluorescence for GFP (green, single channel image (A)), insulin (red, single channel image (B)) and E-Cadherin (gray, single channel image (C)) on sections of *Sox17*$^{CreERT2/+}$ *Rosa*$^{YFP/+}$ E14.5 embryos shows the recombination when tamoxifen is injected at E10.5.Insulin secreting cells (yellow arrows , magnification (E)) in the E14.5 pancreas were not recombined. Pannel (E) represents a magnification of the dashed area in (D). Nuclei are counterstained with DAPI (blue). Abbreviations: dp - dorsal pancreas. Scale bars - 100 µm.

Overall, these experiments confirm that the new *Sox17*^{CreERT2} mouse line is inducible upon tamoxifen injection and expresses *Cre* in the expected cell types (Table 3.1). Furthermore, we showed that recombination in the *Rosa26* locus is very efficient in the endoderm when tamoxifen is administered at E6.5 and E7.5, as in these conditions most cells in the endoderm expressed YFP. Recombination can also be induced in precursors of the vascular endothelial lineage as well as in the bile duct. The spatiotemporal induction of Cre in this line allows genetic lineage tracing of distinct *Sox17*$^{+}$ populations, as well as tissue-specific gene edition.

As stated previously, the *Sox17* gene is disrupted in this *Sox17Cre*^{ERT2} line. It has been shown that this haploinsufficiency may be an issue depending of the genetic background of the animals. In a C57BL/6 background, 90% of the *Sox17*$^{+/-}$ mice suffer perinatal lethality due to aberrant development of the liver, gallbladder and bile duct network. The same study reported that in the ICR background a mild phenotype of gallblader hypoplasia is observed only in adults[58]. This new *Sox17*^{CreERT2} line is bred on an ICR background. We did not observe obvious defects; the mice could reach adulthood and were fertile. However, when performing additional mutations this must be taken into account, as it may have an unpredictable effect.

On the other hand, this same characteristic raises the possibility to perform interesting experiments regarding the fate of *Sox17* deficient cells, which has been only briefly explored to date[59].

Table 3.1. Summary of characterization of the Sox17^{CreERT2} line

Time of Injection	Cells recombined		
	VE	DE	Vasculature
E7.5	minimal	variable, usually higher on posterior	minimal
E6.5-7.5	minimal	yes (80-90%)	minimal
E10.5	none	bile duct	yes (~80%)

3.2. Expression of molecular markers in the gut

To determine the effect of the absence of BMP signalling on the dorso-ventral patterning of the endoderm, the organ domain will be assessed at E10.5 using molecular markers. At this time point, morphological features are present only for some organs *e.g.* lungs, the pancreas and the liver. A series of organ-specific markers were selected based on their early expression in the different endoderm-derived organ domains (Table 3.1). The immunohistofluorescence protocol for every marker was optimized on E10.5 wild-type (WT) embryos both for whole-mount staining and on sections. The subsequent figures show the results of the optimization on sections.

Table 3.2. Molecular markers expressed in the primitive gut and assessed in this study

Molecular maker	Region	Onset of expression
NKX2.1	thyroid, lungs, trachea	8.5 [60]
SOX2	esophagus	9.5[61]
FOXN1	thymus	11[62]
GCM2	parathyroid	9.5[62]
PROX1	liver	8.5[63]
HLXB9	dorsal gut, pancreas	8.0[64]
PITX2	caecum	11[65]

3.2.1. Nkx2.1 and Sox2

Nkx2.1 and *Sox2* encode transcription factors that inhibit each other's expression. Therefore, their expression is mutually exclusive in different domains of the foregut. They are necessary for the proper formation of the trachea and the esophagus, respectively[37,61]. NKX2.1 is expressed in the ventral foregut endoderm as well as in the lungs and the thyroid, as was observed in E10.5 WT embryos (Figure 3.6). Wholemount stainings of the thyroid and lungs were also successful (Supplementary video 1 and 2). Complementary to the ventral expression of NKX2.1, high levels of SOX2 marked the dorsal foregut endoderm (Figure 3.7). SOX2 expression was also detected at lower levels in the main bronchi (Figure 3.7 - B, C). Indeed, this transcription factor has been shown to inhibit lung branching and its overexpression in the respiratory epithelium causes a severe reduction in the number of airways[66].

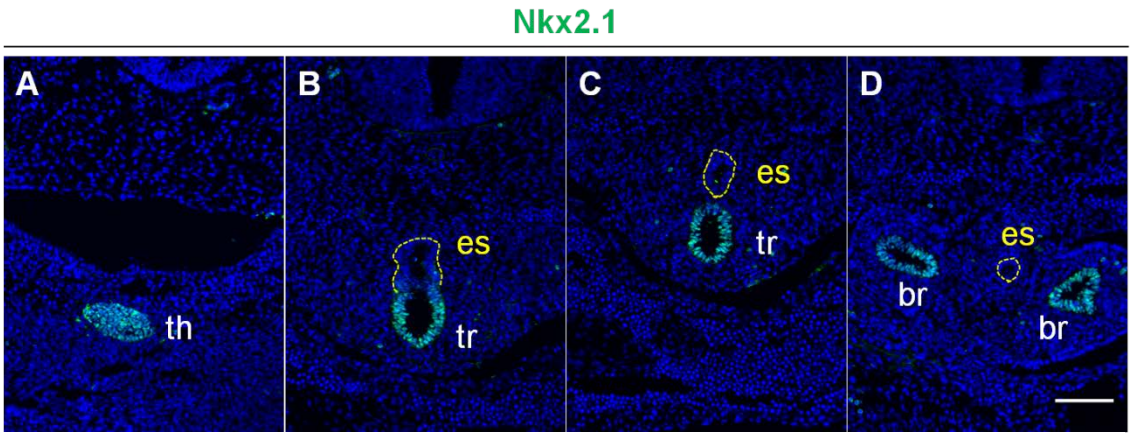

Figure 3.6. NKX2.1 in WT E10.5 embryos. (A-D) Immunofluorescence for NKX2.1 (green) was performed on WT E10.5 embryonic sections. NKX2.1 is found in the thyroid (A) in the trachea (B,C) and in the main bronchi (D). The esophagus can be morphologically distinguished and do not expressed NKX2.1 (B, C, D - yellow lines). Nuclei are counterstained with DAPI (blue). Abbreviations: th - thyroid; es - esophagus; tr - trachea; br - bronchi. Dorsal is towards the top and ventral towards the bottom. Scale bar - 100 µm.

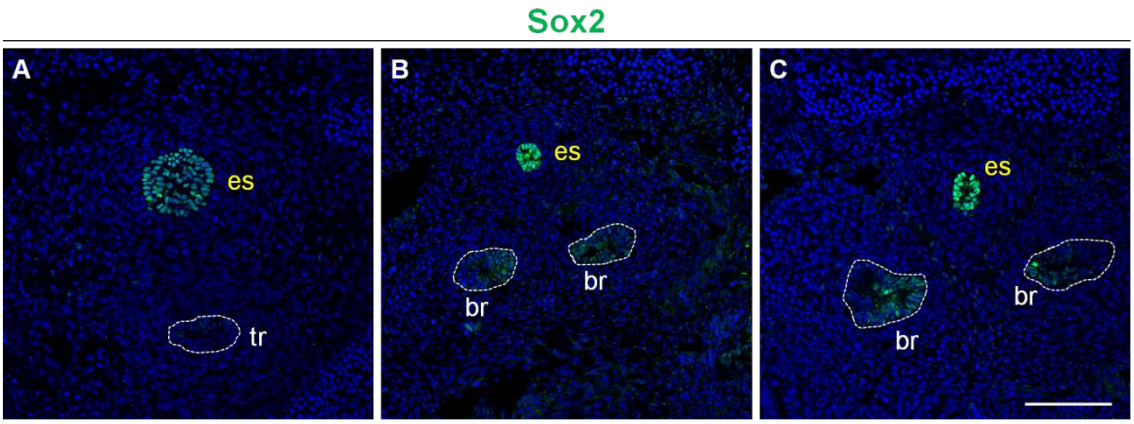

Figure 3.7. SOX2 in WT E10.5 embryos. (A-C) Immunofluorescence for SOX2 (green) was performed on WT E10.5 embryonic sections. SOX2 is found in the esophagus. Trachea can be morphologically distinguished (white lines) (A) as well as the main bronchi (B, C). SOX2 is found at lower levels in the main bronchi (C). Nuclei are counterstained with DAPI (blue). Abbreviations: es - esophagus; tr - trachea; br - bronchi. Dorsal is towards the top and ventral towards the bottom. Scale bar - 100 µm.

3.2.2. Gcm2 and Foxn1

The thymus and parathyroid glands originate from the same endodermal primordium and develop bilaterally, in the third branchial pouch. In the adult, the thymus is situated above the heart and is responsible for T cell production, whereas the parathyroids are found near the thyroid and regulate calcium homeostasis. By E9.5 the thymus and parathyroid start to be specified, but they cannot be morphologically

distinguished at this point. GCM2 marks the dorsal region in the common primordium which later becomes the parathyroid (Figure 3.8), while *Foxn1* is expressed in the ventral domain that originates the thymus. However its expression only starts at E11 making it less suitable for this study[62]. Wholemount stainings of the parathyroid was also successful (Supplementary video 3).

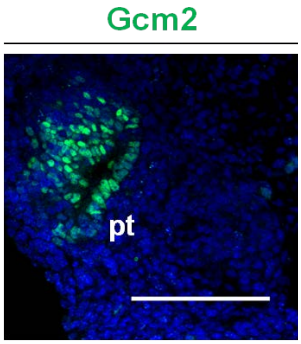

Figure 3.7. GCM2 in WT E10.5 embryos. Immunofluorescence for GCM2 (green) was performed on WT E10.5 embryonic sections. GCM2 is found in a small domain located dorsally on the third branchial pouch, where the parathyroid will develop. Nuclei are counterstained with DAPI (blue). Abbreviations: pt - parathyroid. Scale bar - 100 µm.

3.2.3. Prox1

PROX1 is found in the liver, in both pancreatic buds and in the bile duct at E10.5 (Figure 3.9). Wholemount stainings of the liver, pancreas and bile duct with Prox1 were also successful (Supplementary video 4). Expression in the liver domain starts at E8.5 and is first observed in the budding dorsal pancreas at E9.5[63].

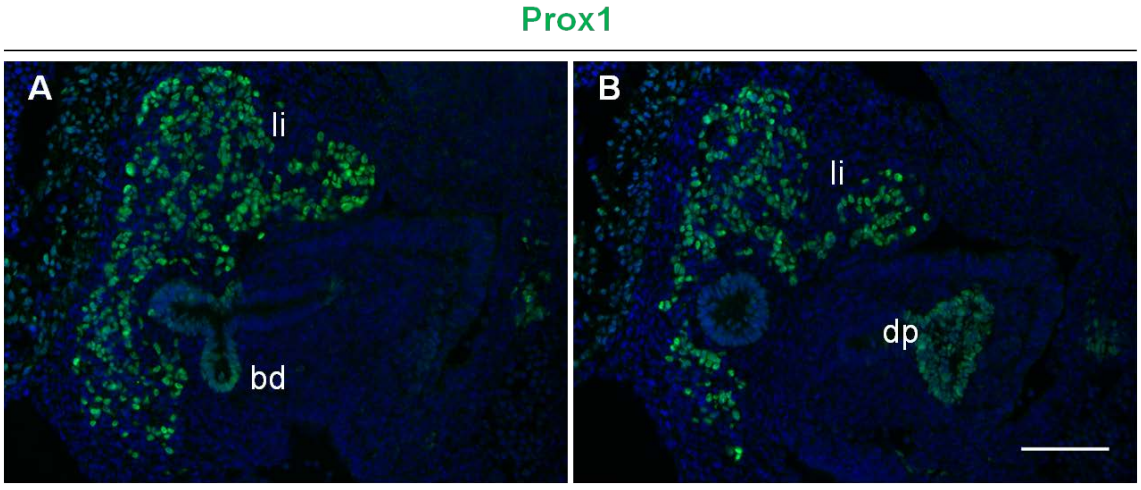

Figure 3.7. PROX1 in WT E10.5 embryos. (A, B) Immunofluorescence for PROX1 (green) was performed on WT E10.5 embryonic sections. PROX1 is found in the liver (A, B), the bile duct (A) and in the pancreatic buds, *e.g.* dorsal pancreatic bud (B). Nuclei are counterstained with DAPI (blue). Abbreviations: bd - bile duct; dp - dorsal pancreas; li - liver. Scale bar - 100 µm.

3.2.4. Hlxb9

HLXB9 is found all along the dorsal wall of the gut epithelium as well as in the dorsal pancreas (Figure 3.10). *Hlxb9* is also expressed transiently in the ventral pancreas. After E10.5, only the differentiating beta-cells and the beta cells expressed *Hlxb9* in the pancreas[64]. Wholemount stainings of with hlxb9 were also successful (Supplementary video 5).

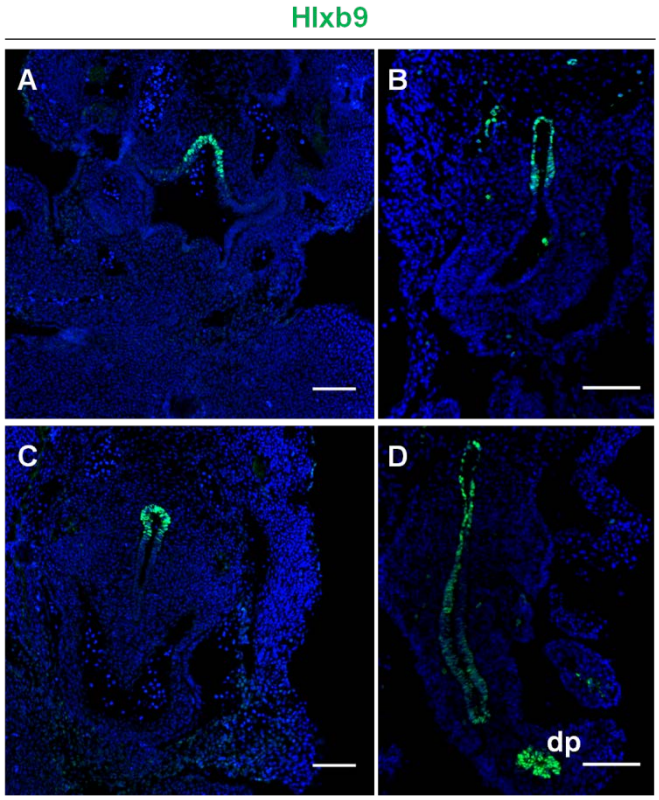

Figure 3.10. HLXB9 in WT E10.5 embryos. (A, B) Immunofluorescence for HLXB9 (green) was performed on WT E10.5 embryonic sections. HLXB9 is found dorsally all along the gut endoderm. (A, B, C). HLXB9 was also found in the dorsal pancreatic bud (D). Nuclei are counterstained with DAPI (blue). Dorsal is towards the top and ventral towards the bottom. Abbreviations: bd - bile duct; dp - dorsal pancreas; li - liver. Scale bars - 100 µm.

3.2.5. Pitx2

Pitx2 is expressed in the epithelium and the mesenchyme of the caecum primordium from E11.0. It is required for the formation of the caecum[67]. Commercial antibodies against PITX2 were tested on E10.5 embryos. However, the different tests did not give any conclusive results. This may result from PITX2 not yet being expressed at this stage or defective antibodies, hypotheses that were not yet tested.

3.2.6. Effectors downstream of BMP: pSMAD1/5/8

In order to monitor BMP pathway activity, we evaluated the presence of a downstream effector, the phosphorylated form of SMAD1/5/8 (pSMAD1/5/8.

pSMAD1/5/8 immunoreactivity should be absent when BMP signalling is inactive. In wild-type E9.5 and E10.5 embryos, pSMAD1/5/8 was observed ventrally in the gut endoderm and in the surrounding mesoderm (Figure 3.11 - A, B). To assess the specificity of the antibody, a phosphatase treatment was performed; in this case no signal was detected in the ventral part of the gut and the surrounding ventral mesoderm (Figure 3.11 - C).

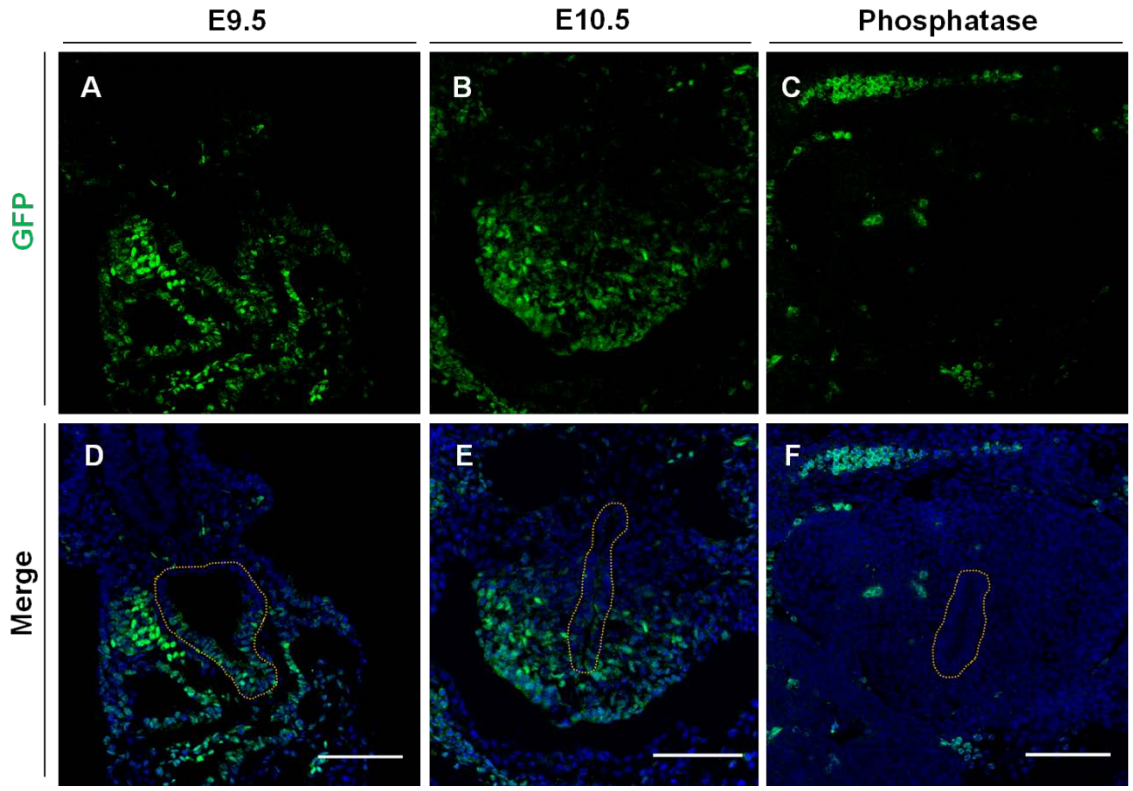

Figure 3.11. pSMAD1/5/8 in WT embryos and phosphatase treatment. (A, B) Immunofluorescence for pSMAD1/5/8 (green, single channel image (A, B, C)) was performed on WT E9.5 (A) and E10.5 (B) embryonic sections. pSMAD1/5/8 staining is found in the ventral region of the gut and the surrounding mesenchyme. (C) Phosphatase treatment followed by immunnofluorescence on sections for pSMAD1/5/8 (green) on E10.5 WT embryos. After treatment with phosphatase, no pSMAD1/5/8 staining is observed, which assures the antibody specificity. Nuclei are counterstained with DAPI (blue). Unspecific signals coming from the blood cells are evident in C. The gut epithelium is outlined. Dorsal is towards the top and ventral towards the bottom. Scale bar - 100 µm.

3.2.7. Sequential immunofluorescence

Multiple antibodies presented in this section are generated in the same species (See Table 2.1 in Materials and Methods). Critically, both HLXB9 and pSMAD1/5/8 antibodies were raised in rabbit. To circumvent this issue, we developed a strategy of sequential immunofluorescence. With this method, two rounds of immunofluorescence staining using antibodies raised in the same species are performed separated by a

stripping procedure which removes the primary and secondary antibodies of the first staining. If a fluorescent precipitate, such as tyramide, is used to detect the first immunofluorescence, it is possible to visualize both signals at the same time as the stripping does not remove the precipitate Therefore, in the presented example, it was possible to image together HLXB9 and pSMAD1/5/8 signals (Figure 3.12).

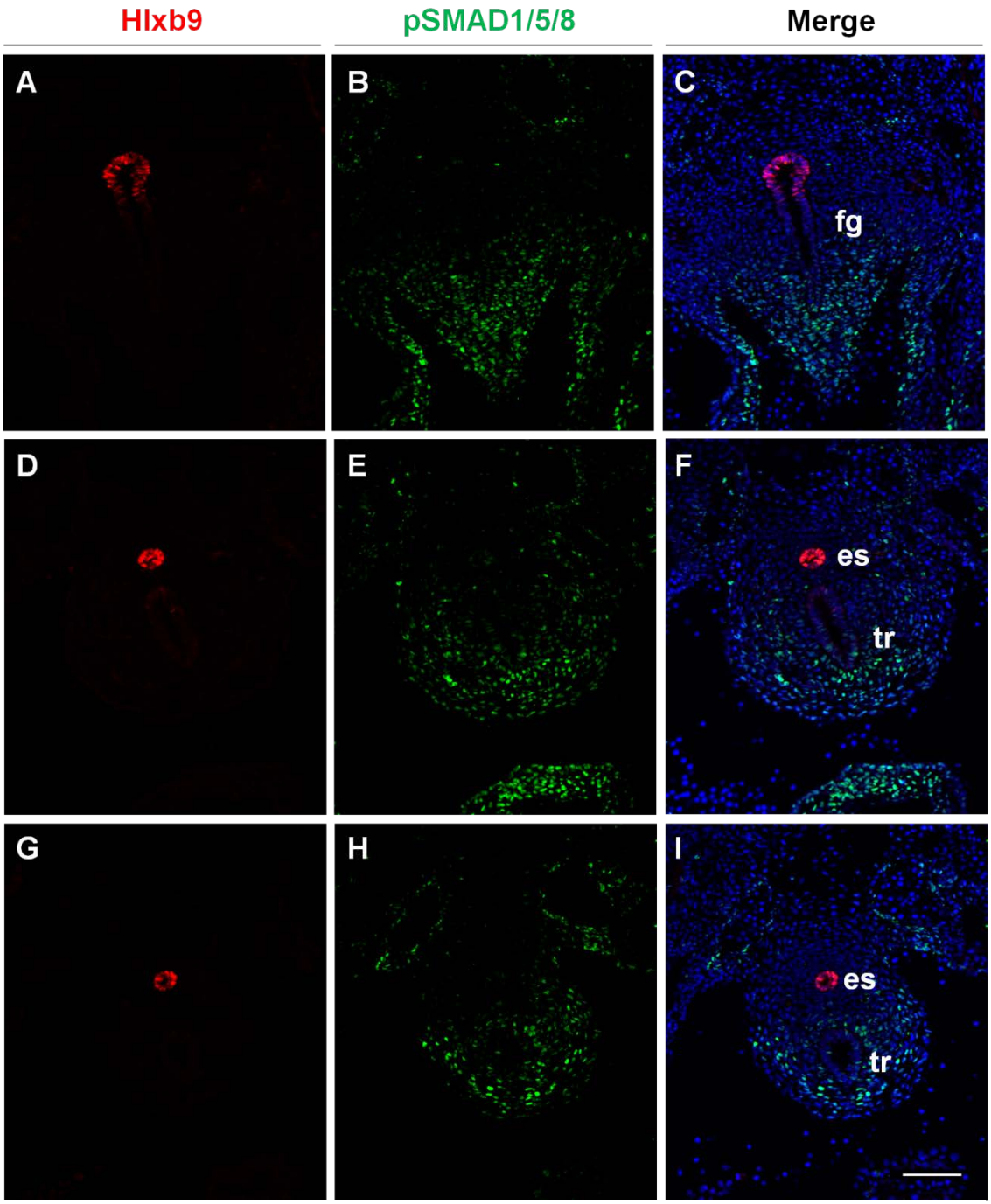

Figure 3.12. pSMAD1/5/8 in a E10.5 embryo after stripping primary antibodies. (C, F, I) Immunofluorescence was performed for HLXB9 (red, single channel image (A, D, G)) on E10.5 embryonic sections using a tyramide dye. This was followed by antibody stripping and subsequent immunofluorescence for pSMAD1/5/8 (green, single channel image (B, E, H)). HlLXB9 is found in the esophagus (red), whereas pSMAD175/8 is found in the ventral gut region (green) (C, F,I). Nuclei are counterstained with DAPI (blue). Dorsal is towards the top and ventral towards the bottom. Abbreviations: fg - foregut; es - esophagus; tr - trachea. Scale bar - 100 µm.

3.3. Inactivation of the BMP pathway

Inactivation of the BMP pathway in the gut endoderm was achieved by conditionally inactivating *Alk3* using the previously characterized *Sox17*^{CreERT2} mouse line, in a null background for *Alk6*. The pathway was thereby permanently inactivated in the progeny of the cells that expressed *Sox17*$^{+}$ at the time of tamoxifen injection in the Sox17$^{creERT2/+}$; Alk3$^{fl/fl}$; Alk6$^{-/-}$embryos (hereafter called dKO). As discussed previously, injection of tamoxifen at E6.5 and E 7.5 in the presented *Cre*^{ERT2} line causes widespread recombination of *Sox17*$^{+}$ DE progenitor cells.

The inactivation of the pathway was achieved via the receptors and not through the ligands. Indeed, BMPs are present in both the endoderm and the surrounding mesenchyme. Their deletions may result in deleterious effects in the mesenchyme, impairing further analysis. Moreover, the receptors are less redundant than the ligands and deletion of both main receptors ALK3 and ALK6 are expected to avoid compensatory mechanisms due to their redundancy.

3.3.1. Inactivation of both receptors is lethal before E10.5

Unexpectedly, double knock-out (dKO) embryos did not survive until E10.5. The effect was not due to tamoxifen toxicity in this background since wild-type and heterozygote littermates were recovered in the expected ratios (Figure 3.13). A single dKO embryo was found, but wholemount analysis suggests that the inactivation of the pathway was likely not achieved in this litter, as none of the littermates presented abnormalities (see subsequent sections and data not shown). Early embryonic lethality is often associated with gastrulation defects. However, the pathway inactivation was induced by injecting tamoxifen after gastrulation has occurred excluding this hypothesis. Due to the time at which BMP inactivation was performed, we suspect that the absence of BMP signalling in the DE at this stage interferes with gut tube closure and embryonic turning, precluding further development. Interestingly, mice with the *Sox17*$^{CreERT2/+}$*; Alk3*$^{fl/fl}$*; Alk6*$^{-/+}$ genotype (hereafter termed Hz) survived until E10.5, indicating that the presence of a single allele of *Alk6* is sufficient to prevent the lethal phenotype observed in the dKO. It is noteworthy that ALK6 is first expressed in the AIP at E7.5[22] suggesting that the absence of BMP signalling in the AIP at around E7.5 causes lethality. The AIP is the place where ventral gut closure begins, indicating that BMP signalling in the DE may be required for ventral closure of the gut. It is supported by the effect of the deletion of Furin, an enzyme responsible for activation of BMP4[18].

Furin knock-out embryos are unable to undergo ventral closure and axial turning[68]. However, it cannot be excluded that *Alk6* compensates the absence of *Alk3* in other parts of the endoderm where ALK6 is normally not required. To verify this hypothesis, the phenotype of dKO embryos should be analysed at earlier stages, such as E8.5. It would also be important to analyse the expression of ALK6 in the Hz embryos before E10.5 to evaluate putative compensatory mechanisms.

We proceeded to analyse the phenotype of Hz mutants by comparing it to wild-type littermates, mainly through wholemount immunofluorescence.

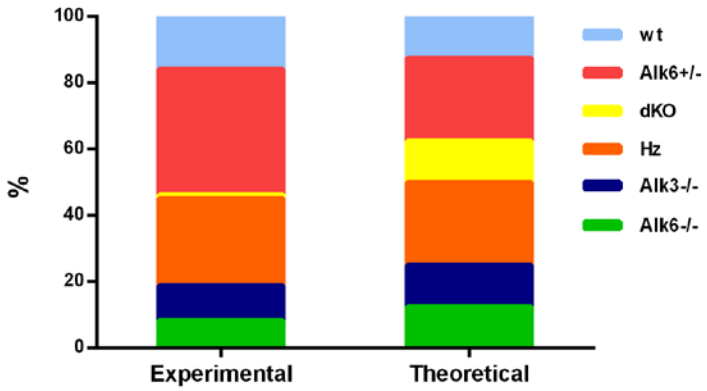

Figure 3.13. Percentages of genotypes obtained overall (A) compared to the theoretical percentages (B) at E10.5. The proportions of genotypes obtained were similar to those expected, with the exception of the dKO, which was lethal.

3.3.2. Hz embryos have several organ development defects

Even though Hz embryos survived until E10.5, they harboured several developmental defects, indicating that lowering BMP activity in the gut is sufficient to disrupt appropriate endoderm-derived organogenesis (Figure 3.14). Moreover, we also noticed that the epithelium of the gut of the Hz mutant looked globally thinner and less compact (Figure 3.14, 3.15, 3.16). It may be due to a proliferation defect occurring in the primitive gut endoderm of the Hz mutant. Accordingly, the absence of BMP4 in the anterior foregut causes a proliferation defect without an increase of cell death[36]. The growth impairment may also be more global as the Hz embryos were smaller than their WT littermates. Thus, it will be important to assess the cell survival and proliferation at E10.5 and earlier to understand this defect.

All Hz embryos analysed by wholemount immunofluorescence (n=3) lacked expression of NKX2.1 (Figure 3.14). While the thyroid, the trachea and lungs were normal in wild-type embryos (Figure3.14 - A), they were not visible in their Hz littermates (Figure3.14 - B). Even though the presence of the thyroid domain was not

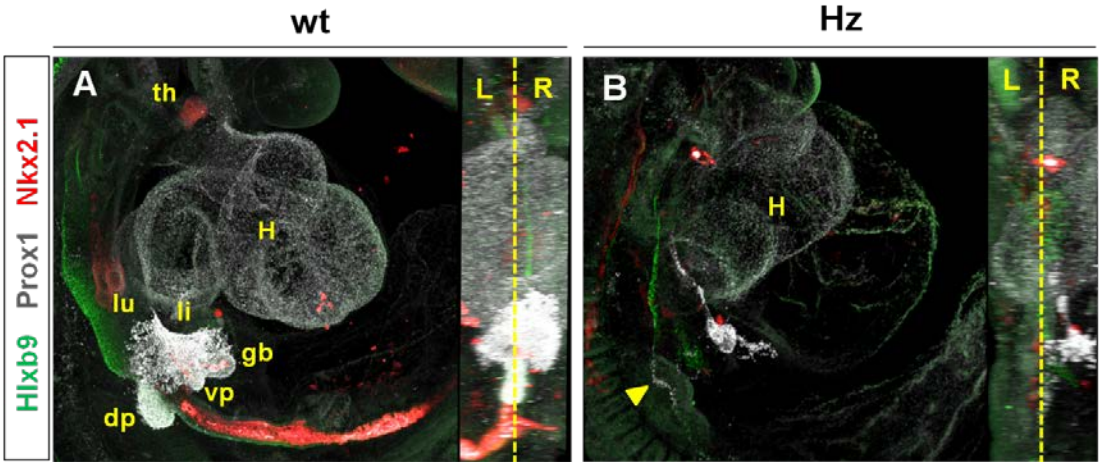

Figure 3.14. Three-dimensional projection of WT and Hz littermates, at E10.5. (A, B) Wholemount immunofluorescence for HLXB9 (green), NKX2.1 (red) and PROX1 (white) in E10.5 WT /A) and Hz (B) embryos after injection of tamoxifen at E6.5 and E7.5. In the WT, NKX2.1 is present in the thyroid and lungs; HLXB9 is present in the dorsal region along the whole gut tube as well as in both pancreatic buds; PROX1 is present in the liver, the gallbladder and in both pancreatic buds (A). In the Hz mutant no NKX2.1 was found; HLXB9 is still present dorsally in the gut tube, but the epithelium seems thinner and deformed; PROX1 is expressed only on the right side of the embryo (B - L|R panel); the ventral pancreas and gallbladder are not evident. PROX1 and HLXB9 are found overlapping dorsally (arrowhead) (B). The strong red signal seen in A is a result of antibodies eing trapped in the lumen of the gut tube. Abbreviations: dp - dorsal pancreas; gn - galbladder; li - liver; lu - lungs; th - thyroid; vp - ventral pancreas; H - heart; L - left; R - right.

investigated with other markers or at a later time point when the primordium is formed, the data suggests that it will not form, since Nkx2.1 is critical for its development[69]. In order to closely observe the structure of the foregut in the Hz mutant, one embryo (n=1) was sectioned after wholemount staining. No lungs or trachea were observed (Figure 3.16 - D). The absence of trachea stained by NKX2.1 in the mutant agrees with the requirement of BMP4 for its development[36]. Previously, disruption of BMP signalling in the foregut after specification had been shown to cause defects in lung development. The lungs formed but were smaller and less branched[37]. However, the inactivation of BMP signalling was performed after specification contrary to our study, in which no lungs are observed suggesting that the BMP pathway is also necessary for lung specification. However, it will be important to analyse the mutant at earlier stages to confirm that BMP signalling is required for lung specification in addition to the maintenance of its identity.

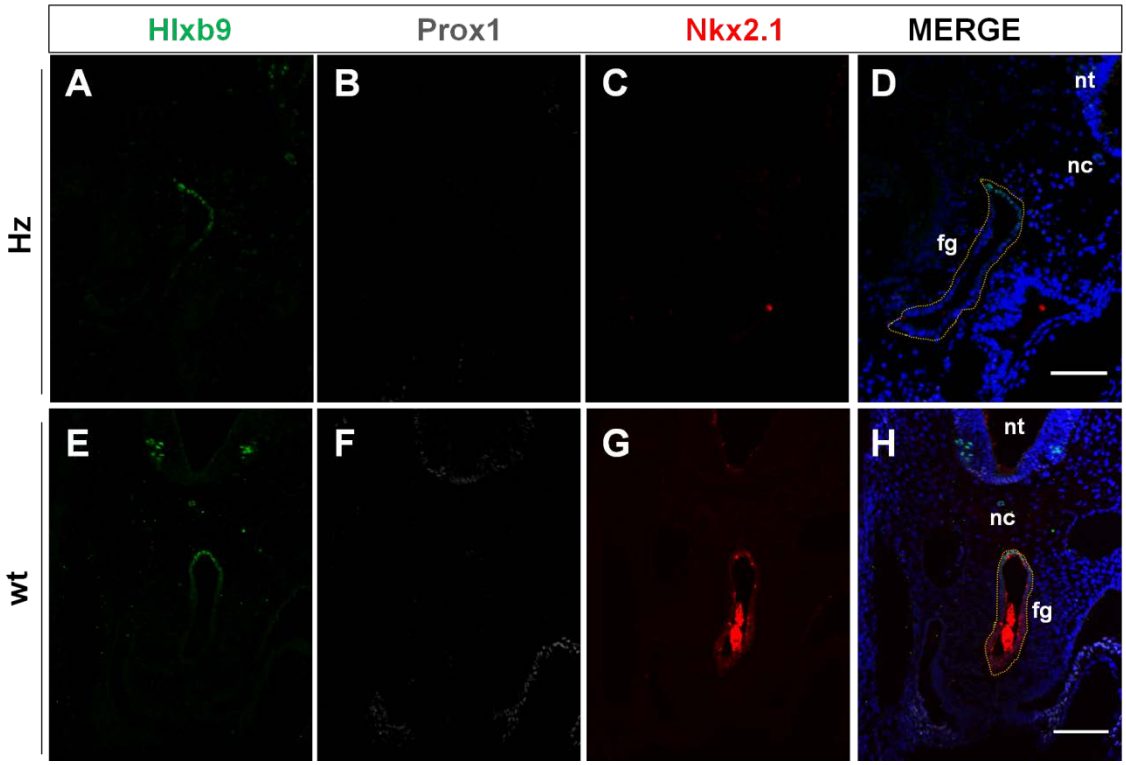

Figure 3.15. . Comparison of foregut in the WT and Hz littermates at E10.5. (D, H) Immunofluorescence for HLXB9 (green, single channel (A, E)), Prox1 (white, single channel (B, F)) and NKX2.1 (red, single channel (C, G)) on E10.5 embryonic sections, after wholemount immunofluorescence. HLXB9 is found in the dorsal region of the gut in both WT and Hz littermates. Expression of HLXB99 is also observable in the neural tube and the notochord (A, E). NKX2.1 is found in the ventral region of the gut in the WT (G) but not in the Hz littermate (C). The overexposed signal in the gut lumen in H is an artefact of wholemount immunofluorescence. Nuclei are counterstained with DAPI (blue). The gut epithelium is outlined. Dorsal is towards the top and ventral towards the bottom. Abbreviations: fg - foregut; nc - notochord; nt - neural tube. Scale bars - 100 µm

At E10.5, PROX1 was expressed in the liver, in both pancreatic buds and in the gallbladder in WT embryos. Moreover, each structure was distinguishable morphologically and the liver already had its characteristic sinusoidal shape (Figure 3.14 A). In the Hz mutant, none of the aforementioned structures was distinguishable (Figure 3.14 B). The position and the arrangement of the cells suggested that the majority of PROX1^{+} cells were hepatocytes, while the rest might have a dorsal pancreatic identity. Nevertheless, more markers should be used in order to assess the identity of the PROX1^{+} cells.

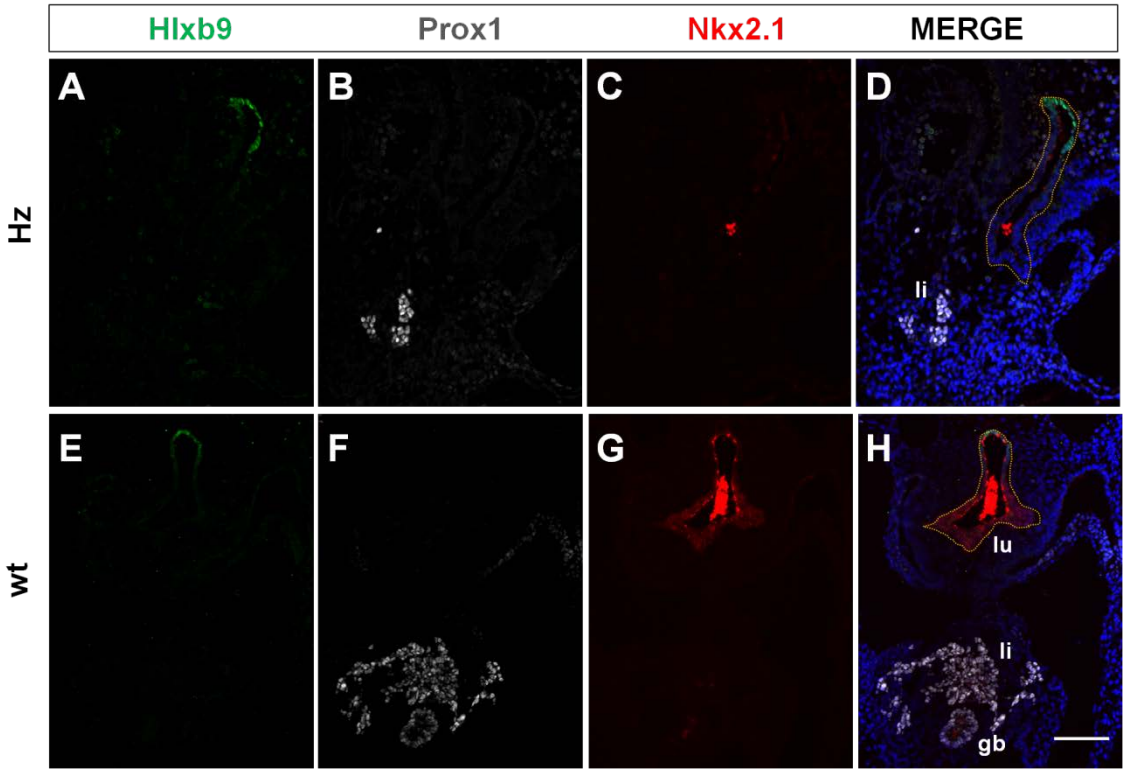

Figure 3.16. Comparison of lung and liver in the WT and Hz littermates at E10.5. (D, H) Immunofluorescence for HLXB9 (green, single channel (A, E)), PROX1 (white, single channel (B, F)) and NKX2.1 (red, single channel (C, G)) on E10.5 embryonic sections, after wholemount immunofluorescence. HLXB9 is found in the dorsal region of the gut in both WT an Hz littermates (A, E). NKX2.1 is found in the ventral region of the gut where the lungs are budding in the WT (G) but not in the Hz littermate (C). PROX1 is expressed both in the WT (F) and in the Hz littermates (B). In the WT different organs can be distinguished by morphological aspects (H - liver/gallbladder). In the Hz however the PROX1 domain is reduced and no evident morphological structures were observed. The overexposed signal in the gut lumen is an artefact of wholemount immunoflourescence. Nuclei are counterstained with DAPI (blue). The gut epithelium is outlined. Dorsal is towards the top and ventral towards the bottom. Abbreviations: gb - gallbladder; li - liver, lu - lungs. Scale bar - 100 µm

PROX1^{+} domain was also drastically reduced. Its total volume was estimated in the Hz mutants and in their WT littermates (n=3) using the Imaris 8.1 software (Figure 3.17). However, slight differences of the embryonic stage at the time of collection cause a high variation in the organ domain size, as organogenesis is fast evolving at these stages. Combined with the small number of cells (Figure 3.14) forming PROX1^{+} domain, it could explain why its

volume might be 6 times higher in the largest compared to the smallest WT of different litters. For this reason the volume of PROX1 in the Hz mutant was normalized to the volume of its WT littermate (Figure 3.18). This analysis revealed that the total PROX1 expression domain is significantly reduced in the Hz mutant.

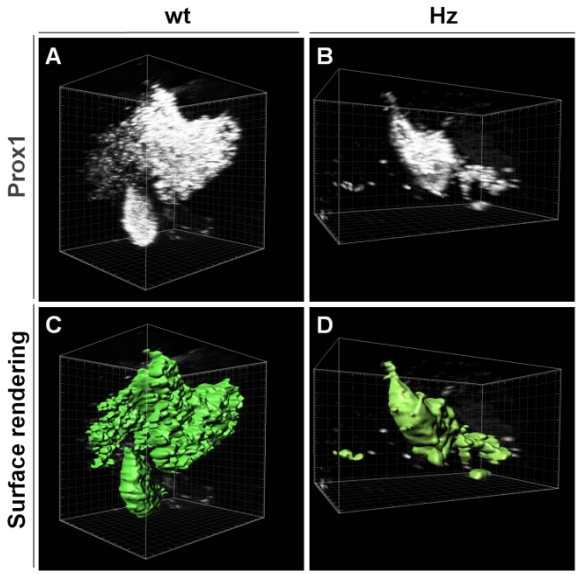

Figure 3.17. Surface rendering of prox1 expression domain. The three dimensional PROX1 domains were isolated from the remaining three dimensional image (white, A, B). Using the Imaris 8.1 software surfaces were rendered based on PROX1 signal (green, C, D). The same settings were replicated for each surface simulation.

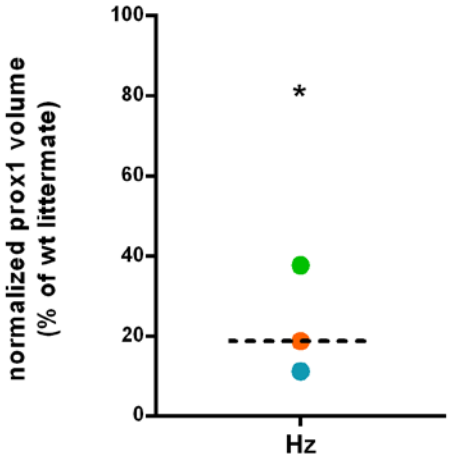

Figure 3.18. Total Prox1 volumes in the Hz embryos (% of WT littermate). The volumes obtained for the Hz mutants through surface rendering in the Imaris software were plotted normalized to the WT volumes (n=3). PROX1 domains are significantly smaller in the Hz mutants than in the WT littermates. Orange - Litter 1; Green - Litter 2; Blue - Litter 3. *One sample t test p=0,01

Before ventral closure, the liver starts developing bilaterally in the lateral endoderm. Both primordia meet and form a single organ when the lateral endoderm migrates ventrally[70]. Interestingly, the putative liver observed in the Hz mutant was located on the right side of the embryo (Figure 3.14 B), suggesting that the specification process of the right and left liver primordia are differently affected by BMP signalling. Furthermore, the pre-cardiac mesoderm which is necessary for the specification of the hepatogenic endoderm also receives reciprocal signals from this tissue to further develop[71]. In the Hz mutant, the heart also appears smaller when visualized with PROX1 staining (Figure 3.14 B). It might be a consequence of lack of reciprocal signalling between the liver and the pre-cardiac mesoderm.

Remarkably, no ventral pancreatic bud was formed in any of the Hz embryos while the outcome of the alteration of BMP signalling on the dorsal pancreatic bud was variable. In one instance, the dorsal pancreas seemed completely absent based on PROX1 and HXLB9 staining. In another litter, there was no apparent budding but PROX1 and HLXB9 expression overlapped dorsally, in the prospective region of the dorsal pancreatic bud (Figure 3.14 B). Finally, in the third litter, a bud was observed, although it was underdeveloped compared to its WT counterpart (Figure 3.19 C, F). The variable dorsal pancreatic phenotype may be linked to a slight difference in the developmental stage of the embryos or to differences in recombination rates between litters. These data indicate that BMP signalling is probably required for the specification of the ventral pancreatic bud while the effect of BMP signalling on dorsal pancreatic bud is less clear but suggest it is required for pancreatic growth, as previously suggested in chick[72].

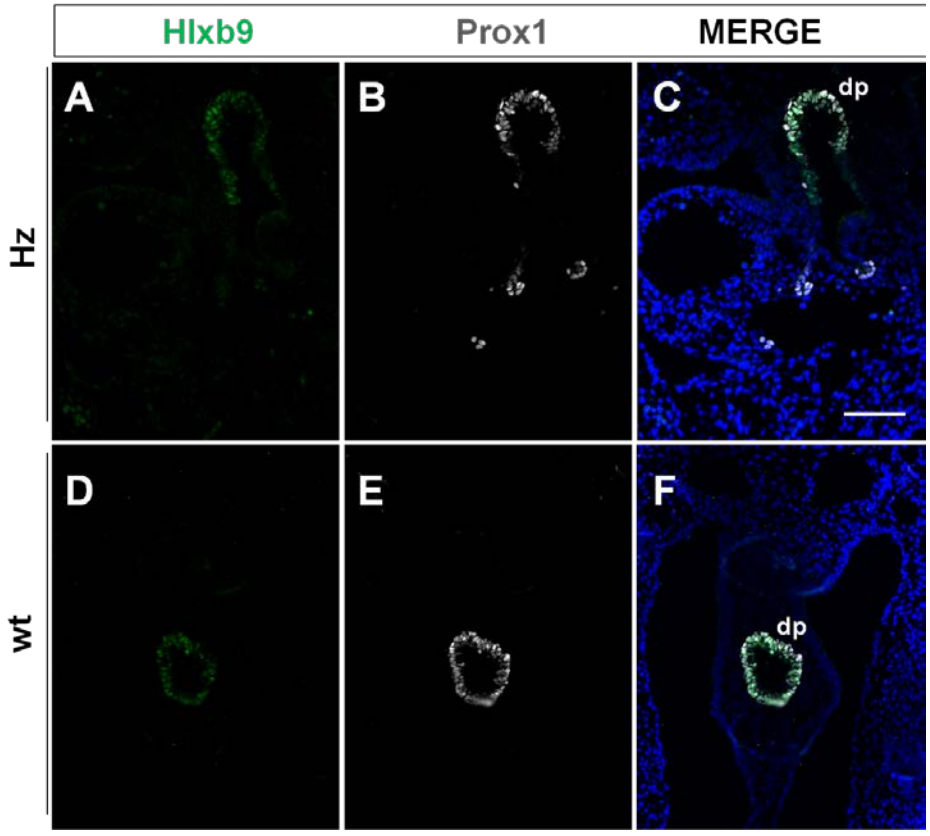

Figure 3.19. Comparison of dorsal pancreas in the WT and Hz littermates at E10.5. (C, F) Immunofluorescence for HLXB9 (green, single channel (A, D)) and PROX1 (white, single channel (B, E)) on E10.5 embryonic sections, after wholemount immunofluorescence. Overlapping domains of HLXB99 and PROX1 as well as the morphology, indicate that the dorsal pancreas is present both in the WT (F) and the Hz mutant (C). Nuclei are counterstained with DAPI (blue). Abbreviations: dp - dorsal pancreas. Scale bar - 100 µm

The global dorsal molecular marker HLXB9 was expressed in the dorsal endoderm of both WT and Hz embryos. Although the size of the domain has not been quantified, it implies that the dorsal identity of the primitive gut tube remains unaffected.

In summary, the resulting phenotype shows that the inactivation of BMP signalling through the ALK3 receptor and partially through the ALK6 receptor disturbs the ventral patterning of the anterior foregut as well as the formation of several organs, including the dorsal pancreas. Globally, the gut epithelium of Hz mutants appears to be thinner and less shapely while the surrounding mesoderm did not seem affected by the alteration of BMP signalling, indicating that conditional deletion of *Alk3* in the endoderm was successful. The heart developmental defect is likely associated to the lack of reciprocal signalling from the liver endoderm, since this organ is significantly reduced.

In this study we provide evidence that the disruption of BMP signalling in the endoderm after onset of gastrulation causes embryonic dead before E10.5. Uncovering the developmental defects that cause death in these embryos will provide further information on the role of BMP signalling in the endoderm during these stages.

Furthermore, the preliminary results on characterization of the Hz phenotype reveal that disturbance of BMP signalling in the endoderm results in global defects in the endoderm. To achieve a deeper understanding of the phenotype of the Hz mutants, several further experiments could be conceived. The extent of BMP signalling inactivation in the Hz mutant should be assessed by evaluating pSMAD1/5/8 levels in the gut, as described in section 3.2.6. This experiment would reveal to which extent endodermal cells have undergone recombination and the level of BMP signalling in other cells. Alternatively, a recombination reporter could be included in the breeding scheme. The analysis of other endoderm-derived organs is also required. Indeed the global ventralizing activity of BMP is unclear since the dorsal pancreatic bud is either hypoplastic or absent and HLXB9 domain does not appear to be extended ventrally. Therefore, in order to assess our hypothesis, it will be important to evaluate the presence of the other dorsal organ, the parathyroid, by analysing the expression of GCM2. In addition, a ventral posterior organ, the caecum, could be assessed by expression of *Pitx2* in the Hz embryo, possibly by *in situ hybridization*. It will also be interesting to examine pancreatic specific markers, such as PTF1A or PDX1, in order to differentiate the liver, the pancreas and the gallbladder. Additional global markers like SOX2 (dorsal foregut) and Islet1 (global ventral in chick, Palle Serup unpublished data) might offer further insight into which targets are affected by BMP signalling. As

our analyses cannot rule out a defect in the maintenance of the identity of the endoderm-derived organs, the Hz mutants should also be studied at earlier stages. A part of the observed phenotype might be associated with a defect in the number of endodermal cells. Thus, the levels of endoderm proliferation and cell death in the Hz mutant should also be evaluated at an early stage such as E8.5.

Chapter IV

Final Remarks

Final Remarks

BMP signalling is essential for many aspects of development, including mesoderm formation and ectoderm patterning. In the DE, several studies have identified roles of BMP signalling in the formation of ventral gut organs [34-38].

We proposed that BMP signalling acts as a global cue in ventral patterning of the DE (Figure 1.3). The findings presented in this study are in accordance with the hypothesis. However, many questions remain before it can be confirmed. For instance, BMP signalling may be essential for the initial invagination of the AIP as suggested previously[73], or it may also be required for ventral migration of the lateral DE and consequent ventral closure of the gut tube. The role of BMP in organogenesis is also still unclear. Is it required for specification, proliferation, maintenance of identity? Perhaps it is required for distinct processes depending on the organ in question. Challenges in the future are to uncover new targets of BMP during endoderm development. Human Embryonic Stem cell derived endoderm could be used in order to identify which genes are downstream targets of BMP.

A global understanding of how BMP signalling acts during dorsal-ventral patterning of the DE will facilitate the development of more efficient protocols that better emulate the development of organs like the lungs, liver or the pancreas, bringing us one step forward into the exciting field of *in vitro* organogenesis[74].

Cited Literature

1. Choi, E.*, et al.* Dual lineage-specific expression of Sox17 during mouse embryogenesis. *Stem cells (Dayton, Ohio)* **30**, 2297-2308 (2012).
2. Grapin-Botton, A. Endoderm Specification. in *StemBook* (ed. Community, T.S.C.R.) (2008).
3. Grapin-Botton, A. & Melton, D.A. Endoderm development: from patterning to organogenesis. *Trends in genetics : TIG* **16**, 124-130 (2000).
4. Balemans, W. & Van Hul, W. Extracellular regulation of BMP signaling in vertebrates: a cocktail of modulators. *Dev Biol* **250**, 231-250 (2002).
5. Zorn, A.M. & Wells, J.M. Vertebrate endoderm development and organ formation. *Annu Rev Cell Dev Biol* **25**, 221-251 (2009).
6. Desrochers, T.M., Palma, E. & Kaplan, D.L. Tissue-engineered kidney disease models. *Adv Drug Deliv Rev* **69-70**, 67-80 (2014).
7. Wang, L.*, et al.* Engineering Three-Dimensional Cardiac Microtissues for Potential Drug Screening Applications. *Curr Med Chem* **21**, 2497-2509 (2014).
8. Patthey, C. & Gunhaga, L. Signaling pathways regulating ectodermal cell fate choices. *Experimental cell research* **321**, 11-16 (2014).
9. Kimelman, D. Mesoderm induction: from caps to chips. *Nat Rev Genet* **7**, 360-372 (2006).
10. Nowotschin, S. & Hadjantonakis, A.-K.K. Cellular dynamics in the early mouse embryo: from axis formation to gastrulation. *Current opinion in genetics & development* **20**, 420-427 (2010).
11. Kwon, G.S., Viotti, M. & Hadjantonakis, A.-K.K. The endoderm of the mouse embryo arises by dynamic widespread intercalation of embryonic and extraembryonic lineages. *Developmental cell* **15**, 509-520 (2008).
12. Viotti, M., Nowotschin, S. & Hadjantonakis, A.-K.K. Afp::mCherry, a red fluorescent transgenic reporter of the mouse visceral endoderm. *Genesis (New York, N.Y. : 2000)* **49**, 124-133 (2011).
13. Spooner, B.S., Walther, B.T. & Rutter, W.J. The development of the dorsal and ventral mammalian pancreas in vivo and in vitro. *J Cell Biol* **47**, 235-246 (1970).
14. Cordier, A.C. & Haumont, S.M. Development of thymus, parathyroids, and ultimobranchial bodies in NMRI and nude mice. *The American journal of anatomy* **157**, 227-263 (1980).
15. Wills, A., Dickinson, K., Khokha, M. & Baker, J.C. Bmp signaling is necessary and sufficient for ventrolateral endoderm specification in Xenopus. *Dev Dyn* **237**, 2177-2186 (2008).
16. Urist, M.R. Bone: formation by autoinduction. *Science* **150**, 893-899 (1965).
17. Wagner, D.O.*, et al.* BMPs: from bone to body morphogenetic proteins. *Sci Signal* **3**, mr1 (2010).
18. Cui, Y., Jean, F., Thomas, G. & Christian, J.L. BMP-4 is proteolytically activated by furin and/or PC6 during vertebrate embryonic development. *EMBO J* **17**, 4735-4743 (1998).
19. Harrison, C.A., Al-Musawi, S.L. & Walton, K.L. Prodomains regulate the synthesis, extracellular localisation and activity of TGF-beta superfamily ligands. *Growth Factors* **29**, 174-186 (2011).

20. Heldin, C.H. & Moustakas, A. Role of Smads in TGFbeta signaling. *Cell Tissue Res* **347**, 21-36 (2012).

21. Mueller, T.D. & Nickel, J. Promiscuity and specificity in BMP receptor activation. *FEBS letters* **586**, 1846-1859 (2012).

22. Danesh, S.M., Villasenor, A., Chong, D., Soukup, C. & Cleaver, O. BMP and BMP receptor expression during murine organogenesis. *Gene expression patterns : GEP* **9**, 255-265 (2009).

23. Winnier, G., Blessing, M., Labosky, P.A. & Hogan, B.L.M. Bone Morphogenetic Protein-4 Is Required for Mesoderm Formation and Patterning in the Mouse. *Genes & Development* **9**, 2105-2116 (1995).

24. Zhang, H.B. & Bradley, A. Mice deficient for BMP2 are nonviable and have defects in amnion chorion and cardiac development. *Development* **122**, 2977-2986 (1996).

25. de Sousa Lopes, S.M.*, et al.* BMP signaling mediated by ALK2 in the visceral endoderm is necessary for the generation of primordial germ cells in the mouse embryo. *Genes & development* **18**, 1838-1849 (2004).

26. Miyazono, K., Kusanagi, K. & Inoue, H. Divergence and convergence of TGF /BMP signaling. *Journal of cellular physiology* **187**, 265-276 (2001).

27. Dewulf, N.*, et al.* Distinct spatial and temporal expression patterns of two type I receptors for bone morphogenetic proteins during mouse embryogenesis. *Endocrinology* **136**, 2652-2663 (1995).

28. Gu, Z.*, et al.* The type I serine/threonine kinase receptor ActRIA (ALK2) is required for gastrulation of the mouse embryo. *Development (Cambridge, England)* **126**, 2551-2561 (1999).

29. Yi, S.E., Daluiski, A., Pederson, R., Rosen, V. & Lyons, K.M. The type I BMP receptor BMPRIB is required for chondrogenesis in the mouse limb. *Development* **127**, 621-630 (2000).

30. Mishina, Y., Hanks, M.C., Miura, S., Tallquist, M.D. & Behringer, R.R. Generation of Bmpr/Alk3 conditional knockout mice. *Genesis (New York, N.Y. : 2000)* **32**, 69-72 (2002).

31. Beppu, H.*, et al.* BMP type II receptor is required for gastrulation and early development of mouse embryos. *Developmental biology* **221**, 249-258 (2000).

32. Holley, S.A. & Ferguson, E.L. Fish are like flies are like frogs: conservation of dorsal-ventral patterning mechanisms. *BioEssays : news and reviews in molecular, cellular and developmental biology* **19**, 281-284 (1997).

33. Liu, A. & Niswander, L. Bone morphogenetic protein signalling and vertebrate nervous system development. *Nature Reviews Neuroscience* **6**, 945-954 (2005).

34. Bleul, C.C. & Boehm, T. BMP signaling is required for normal thymus development. *Journal of immunology (Baltimore, Md. : 1950)* **175**, 5213-5221 (2005).

35. Frisbie, T.*, et al.* Determining the effect of BMP signaling on thymus fate specification and differentiation of the third pharyngeal pouch in the mouse. (HEM7P.235). *The Journal of Immunology* **194**, 188.115 (2015).

36. Li, Y., Gordon, J., Manley, N.R., Litingtung, Y. & Chiang, C. Bmp4 is required for tracheal formation: a novel mouse model for tracheal agenesis. *Developmental biology* **322**, 145-155 (2008).

37. Domyan, E.T.*, et al.* Signaling through BMP receptors promotes respiratory identity in the foregut via repression of Sox2. *Development (Cambridge, England)* **138**, 971-981 (2011).

38. Rossi, J.M., Dunn, N.R., Hogan, B.L. & Zaret, K.S. Distinct mesodermal signals, including BMPs from the septum transversum mesenchyme, are required in combination for hepatogenesis from the endoderm. *Genes & development* **15**, 1998-2009 (2001).

39. Gouon-Evans, V.*, et al.* BMP-4 is required for hepatic specification of mouse embryonic stem cell-derived definitive endoderm. *Nature biotechnology* **24**, 1402-1411 (2006).

40. Lefebvre, V., Dumitriu, B., Penzo-Méndez, A., Han, Y. & Pallavi, B. Control of cell fate and differentiation by Sry-related high-mobility-group box (Sox) transcription factors. *The international journal of biochemistry & cell biology* **39**, 2195-2214 (2007).

41. Chazaud, C., Yamanaka, Y., Pawson, T. & Rossant, J. Early lineage segregation between epiblast and primitive endoderm in mouse blastocysts through the Grb2-MAPK pathway. *Developmental cell* **10**, 615-624 (2006).

42. Kanai-Azuma, M.*, et al.* Depletion of definitive gut endoderm in Sox17-null mutant mice. *Development* **129**, 2367-2379 (2002).

43. Pfister, S.*, et al.* Sox17-dependent gene expression and early heart and gut development in Sox17-deficient mouse embryos. *Int J Dev Biol* **55**, 45-58 (2011).

44. Corada, M.*, et al.* Sox17 is indispensable for acquisition and maintenance of arterial identity. *Nat Commun* **4**, 2609 (2013).

45. Clarke, R.L.*, et al.* The expression of Sox17 identifies and regulates haemogenic endothelium. *Nat Cell Biol* **15**, 502-510 (2013).

46. Uemura, M.*, et al.* Fate mapping of gallbladder progenitors in posteroventral foregut endoderm of mouse early somite-stage embryos. *The Journal of veterinary medical science / the Japanese Society of Veterinary Science* **77**, 587-591 (2015).

47. Sternberg, N., Sauer, B., Hoess, R. & Abremski, K. Bacteriophage P1 cre gene and its regulatory region. Evidence for multiple promoters and for regulation by DNA methylation. *Journal of molecular biology* **187**, 197-212 (1986).

48. Deng, C.-X. The Use of Cre–loxP Technology and Inducible Systems to Generate Mouse Models of Cancer. *Genetically Engineered Mice for Cancer Research*, 17-36 (2012).

49. Engert, S., Liao, W.P., Burtscher, I. & Lickert, H. Sox17-2A-iCre: a knock-in mouse line expressing Cre recombinase in endoderm and vascular endothelial cells. *Genesis* **47**, 603-610 (2009).

50. Engert, S., Burtscher, I., Kalali, B., Gerhard, M. & Lickert, H. The Sox17CreERT2 knock-in mouse line displays spatiotemporal activation of Cre recombinase in distinct Sox17 lineage progenitors. *Genesis* **51**, 793-802 (2013).

51. Srinivas, S.*, et al.* Cre reporter strains produced by targeted insertion of EYFP and ECFP into the ROSA26 locus. *BMC Developmental Biology* **1**, 4 (2001).

52. van den Brand, M.*, et al.* Sequential immunohistochemistry: a promising new tool for the pathology laboratory. *Histopathology* **65**, 651-657 (2014).

53. Viotti, M., Nowotschin, S. & Hadjantonakis, A.K. SOX17 links gut endoderm morphogenesis and germ layer segregation. *Nat Cell Biol* **16**, 1146-1156 (2014).

54. Reinert, R.B.*, et al.* Tamoxifen-Induced Cre-loxP Recombination Is Prolonged in Pancreatic Islets of Adult Mice. *PLoS One* **7**, e33529 (2012).

55. Robinson, S.P., Langan-Fahey, S.M., Johnson, D.A. & Jordan, V.C. Metabolites, pharmacodynamics, and pharmacokinetics of tamoxifen in rats and mice compared to the breast cancer patient. *Drug Metab Dispos* **19**, 36-43 (1991).

56. Jonatan, D.*, et al.* Sox17 regulates insulin secretion in the normal and pathologic mouse beta cell. *PLoS One* **9**, e104675 (2014).

57. Herrera, P.L.*, et al.* Embryogenesis of the murine endocrine pancreas; early expression of pancreatic polypeptide gene. *Development* **113**, 1257-1265 (1991).

58. Uemura, M.*, et al.* Sox17 haploinsufficiency results in perinatal biliary atresia and hepatitis in C57BL/6 background mice. *Development (Cambridge, England)* **140**, 639-648 (2013).

59. Viotti, M., Nowotschin, S. & Hadjantonakis, A.-K.K. SOX17 links gut endoderm morphogenesis and germ layer segregation. *Nature cell biology* (2014).

60. Serls, A.E., Doherty, S., Parvatiyar, P., Wells, J.M. & Deutsch, G.H. Different thresholds of fibroblast growth factors pattern the ventral foregut into liver and lung. *Development* **132**, 35-47 (2005).

61. Que, J.*, et al.* Multiple dose-dependent roles for Sox2 in the patterning and differentiation of anterior foregut endoderm. *Development* **134**, 2521-2531 (2007).

62. Gordon, J., Bennett, A.R., Blackburn, C.C. & Manley, N.R. Gcm2 and Foxn1 mark early parathyroid-and thymus-specific domains in the developing third pharyngeal pouch. *Mechanisms of development* **103**, 141-143 (2001).

63. Burke, Z. & Oliver, G. Prox1 is an early specific marker for the developing liver and pancreas in the mammalian foregut endoderm. *Mechanisms of Development* **118**, 147-155 (2002).

64. Li, H., Arber, S., Jessell, T.M. & Edlund, H. Selective agenesis of the dorsal pancreas in mice lacking homeobox gene Hlxb9. *Nat Genet* **23**, 67-70 (1999).

65. Nichol, P.F. & Saijoh, Y. Pitx2 is a critical early regulatory gene in normal cecal development. *The Journal of surgical research* **170**, 107-111 (2011).

66. Gontan, C.*, et al.* Sox2 is important for two crucial processes in lung development: branching morphogenesis and epithelial cell differentiation. *Developmental biology* **317**, 296-309 (2008).

67. Burns, R.C.*, et al.* Requirement for fibroblast growth factor 10 or fibroblast growth factor receptor 2-IIIb signaling for cecal development in mouse. *Developmental biology* **265**, 61-74 (2004).

68. Roebroek, A.J.*, et al.* Failure of ventral closure and axial rotation in embryos lacking the proprotein convertase Furin. *Development* **125**, 4863-4876 (1998).

69. Fagman, H. & Nilsson, M. Morphogenetics of early thyroid development. *Journal of molecular endocrinology* **46**, 42 (2011).

70. Tremblay, K.D. & Zaret, K.S. Distinct populations of endoderm cells converge to generate the embryonic liver bud and ventral foregut tissues. *Dev Biol* **280**, 87-99 (2005).

71. Alsan, B.H. & Schultheiss, T.M. Regulation of avian cardiogenesis by Fgf8 signaling. *Development* **129**, 1935-1943 (2002).

72. Ahnfelt-Rønne, J., Ravassard, P., Pardanaud-Glavieux, C., Scharfmann, R. & Serup, P. Mesenchymal bone morphogenetic protein signaling is required for normal pancreas development. *Diabetes* **59**, 1948-1956 (2010).

73. Madabhushi, M. & Lacy, E. Anterior visceral endoderm directs ventral morphogenesis and placement of head and heart via BMP2 expression. *Developmental cell* **21**, 907-919 (2011).

74. Marx, V. Tissue engineering: Organs from the lab. *Nature* **522**, 373-377 (2015).